by

#### PETER ACCOLA

(Under the Direction of James D. Lauderdale and K. Paige Carmichael)

#### **ABSTRACT**

Heterozygous deficiency in the Pax6 gene results in the analogous condition of aniridia in humans and small eye (Sey) in mice. The underlying pathogenesis is incompletely understood. An *in vivo*, murine, corneal wounding model was developed to study healing capacity, evaluate the limbal progenitor cell population (p63), and explore the role of soluble vascular endothelial growth factor receptor-1 (sVEGFR-1) in aniridia related keratopathy. Results demonstrated a statistically significant delay in corneal wound healing in Sey mice at days 2 and 3 when compared to WT mice (p<0.05). There was no significant difference in corneal p63 staining (p>0.05). All corneas exhibited comparable sVEGFR-1 staining. In conclusion, our *in vivo* wounding model revealed delayed corneal healing in Sey mice that does not appear to be due to deficiency in p63 cellular expression. The comparable expression of sVEGFR-1 suggests that it alone is likely not responsible for corneal vascularization present in Sey mice.

INDEX WORDS: Aniridia related keratopathy, Pax6, Cornea, Aniridia, *in vivo*, p63, sVEGFR-1. Wound

# EVALUATION OF CORNEAL HEALING, LIMBAL PROGENITOR CELLS, AND ${\sf VASCULARIZATION\ IN\ PAX\ 6^{+/+}\ AND\ PAX\ 6^{+/-}\ MICE}$

by

### PETER ACCOLA

B.S., University of Wisconsin – River Falls, 1997

 $D.V.M.,\,University\,\,of\,\,Wisconsin-Madison,\,2001$ 

A Thesis Submitted to the Graduate Faculty of The University of Georgia in Partial Fulfillment of the Requirements for the Degree

MASTER OF SCIENCE

ATHENS, GEORGIA

2009

© 2009

Peter Accola

All Rights Reserved

# EVALUATION OF CORNEAL HEALING, LIMBAL PROGENITOR CELLS, AND ${\sf VASCULARIZATION\ IN\ PAX\ 6^{+/+}\ AND\ PAX\ 6^{+/-}\ MICE}$

by

## PETER ACCOLA

Major Professors: James D. Lauderdale

K. Paige Carmichael

Committee: Phillip A. Moore

Angela E. Ellis

Electronic Version Approved:

Maureen Grasso Dean of the Graduate School The University of Georgia December 2009

## DEDICATION

This work is dedicated to my beautiful wife and our family to come.

## **ACKNOWLEDGEMENTS**

I would like to thank my wonderful committee members for their encouragement and dedication. Your direct influence is inextricably linked to this project. I also am grateful to Abbie Butler, Lynn Reece, Nadia Gadsden, and Rob Miller for their technical contributions. I thank my wife, Laurie, for her unwavering support and valuable discussion. Finally I wish to recognize my parents, James and Ida Accola. The foundation you provided guides me daily.

## TABLE OF CONTENTS

	Page
ACKNOWLEDGEMENTS	v
CHAPTER	
1 INTRODUCTION AND LITERATURE REVIEW	1
2 ANTERIOR SEGMENT PATHOLOGY AND CORNEAL WOUND	
HEALING IN PAX6 HETEROZYGOTE MICE	5
INTRODUCTION AND OBJECTIVE	5
MATERIALS AND METHODS	6
RESULTS	11
DISCUSSION	15
REFERENCES	21
FIGURES	34
3 CONCLUSION	61

#### CHAPTER 1

#### INTRODUCTION and LITERATURE REVIEW

Ocular development depends on an organized interaction of tissues from different embryologic origins. This process proceeds in a predictable and stepwise fashion under the control of various transcription factors and induction signals which direct coordinated differentiation of all ocular structures [1]. Alterations in the delicate balance of these controlling factors results in abnormal ocular development.

The Pax multigene family is a group of transcription factors that are responsible for the development of numerous tissues [2]. Pax6, in addition to its contributions to brain, olfactory, and pancreatic formation, plays a principal role in ocular development [3-16]. This gene has been highly conserved in species throughout evolution. A heterozygous loss-of-function mutation in the Pax6 gene results in a congenital ocular condition in humans termed aniridia and a Small Eye (Sey) phenotype in rodents. These two conditions are widely considered homologous given their genotypic and phenotypic similarities [6, 11, 17-35]. In addition to its importance in the developing embryo, Pax6 also plays a regulatory role within the eye postnatally [29, 36, 37].

Aniridia is a panocular developmental disorder that affects the cornea, anterior chamber, iris, lens, retina, and optic nerve [38-41]. Aniridia related keratopathy (ARK) denotes the complex pathology observed in the cornea of both humans with aniridia and in Sey mice. In humans, the cornea develops a peripheral keratopathy which advances towards the central cornea with age [42]. The progressive nature of ARK results in

devastating consequences for vision in these patients. Despite important advances in the understanding of its pathophysiology, the cause of ARK remains elusive [35]. Deficiency in the limbal stem cell population has been proposed as a cause based on, among other things, corneal conjunctivalization [38, 43-47]; however evaluation of cell proliferation and epithelial progenitor cell markers suggest an adequate stem cell population [48]. The prominent corneal neovascularization is thought to be due to deficiency in a soluble receptor for vascular endothelial growth factor A (VEGF-A) in the cornea called soluble VEGF receptor-1 (sVEGFR-1, also known as sflt-1) [49-51]. Additional proposed mechanisms of ARK include abnormal corneal wound healing characterized by an increased epithelial cell fragility secondary to abnormal expression of cytokeratin 12 [48, 52-54], glycosaminoglycan down regulation with resultant deleterious effects on epithelial cell migration [55], defective calcium signaling in Pax6<sup>+/-</sup> cells [56]. and abnormal remodeling of the corneal extracellular matrix [57]. Furthermore, a positive correlation has been made between the severity of ARK and abnormal tear film stability and meibomian gland dysfunction [58]. More recently, an increased susceptibility of the Sey cornea to oxidative stress was shown to result in metaplastic epithelial changes and opacity [59]. Finally, a study of corneal innervation in Sey mice did not support neurogenic keratitis as a cause for ARK [60]. It is clear, therefore, that the underlying mechanism of ARK is multifactorial.

Current treatment options for ARK include penetrating keratoplasty and keratolimbal grafting techniques; however success rates have generally been poor with recurrent keratopathy in grafted tissue [12, 13, 61-64]. Protection of the cornea with long term bandage contact lens [65] or surface lubricants [66] may improve outcome.

Identification of the mechanisms underlying ARK will be important in determining effective future treatments. Ultimately, techniques employing transplantation of genetically repaired Pax6 stem cells may be necessary for definitive treatment [67, 68]. The corneal abnormalities seen in Sey mice provide a useful model for study of ARK in humans [6, 53].

The vast majority of studies evaluating corneal biology in ARK have employed *in vitro* murine models in which wounding is performed in epithelial cell culture, or in which wounding is followed by enucleation and placement of the eye in organ culture. However, these studies have resulted in discordant results of corneal wound healing capacity in Sey mice [55, 69, 70]. This is likely because *in vitro* studies cannot provide the complex cues that *in vivo* cells must integrate. Corneal wounding initiates a series of coordinated events that serve to maintain its refractive and protective functions. Optimal healing involves interaction of not only the resident cells of the cornea and immune system, but contributions from lacrimal glands, conjunctiva, meibomian glands, eyelids, and the afferent and efferent nervous system. This integrated concept of the ocular surface as a functional unit highlights the complexities inherent to corneal wound healing [71, 72]. An *in vivo* study would incorporate the necessary components important in corneal wound healing and thus identify a basal healing capacity in Sey mice from which further work can be compared.

Thus, the objective of this study is to establish and evaluate a prospective, *in vivo* corneal wounding model in Sey mice to aid in future study of the pathophysiology and potential treatment of ARK. This model will then be used to compare corneal wound healing characteristics in Wild Type (WT) and Sey mice, evaluate changes over time in

the limbal progenitor cell population (p63) after wounding, and explore the role of sVEGFR-1 in the vascularization of ARK.

#### CHAPTER 2

## ANTERIOR SEGMENT PATHOLOGY AND CORNEAL WOUND HEALING IN PAX6 HETEROZYGOTE MICE

## 1. Introduction and objective

Corneal wound healing involves a complex interaction of all required components in order to achieve the exquisite clarity which is necessary for normal vision. Heterozygous deficiency in Pax6, a gene important to the development and postnatal function of the eye, results in the analogous condition of aniridia in humans and small eye (Sey) in mice. Humans with aniridia suffer from progressive corneal pathology termed aniridia related keratopathy (ARK) for which the Sey mouse is a model. The underlying mechanisms of ARK are unclear, but may include deficiency in the limbal progenitor cell population and disturbance of factors involved in maintaining corneal avascularity. The hypothesis of this study is that the Pax6 heterozygote genotype will result in defective corneal wound healing, a deficiency in limbal progenitor cells, and impairment of corneal anti-angiogenesis. The objective of this study is twofold. First, we will establish a prospective, in vivo corneal wounding model in Sey mice for future study of the pathophysiology, and potential treatment, of ARK. Second, this model will be used to determine corneal wound healing capacity in Wild Type (WT) and Sey mice, compare their limbal progenitor cell population (p63), and explore the role of a VEGF-A receptor (sVEGFR-1) in the vascularization of ARK.

#### 2. Materials and Methods

## 2.1. Experimental Animals

A total of 79 Pax6<sup>+/+</sup> (CD1; Charles River Laboratories) and 40 Sey<sup>Neu</sup> (Pax6<sup>+/-</sup>) mice on CD1 background (J.D. Lauderdale murine breeding colony, Department of Cellular Biology, University of Georgia, Athens, GA) between the ages of 8 and 12 weeks were included in this study. Heterozygous Pax6<sup>+/-</sup> mice were produced from crosses between WT (CD1 x CD1) F1 females and Pax6<sup>+/-</sup> wales on a CD1 background. Housing consisted of mice separated by sex in cages within a controlled room temperature (20°C - 22°C), humidity (33-48%), and a constant 12 hour light – dark cycle. Mice had access to free choice water and were fed Laboratory Rat Diet 5001 (LabDiet<sup>®</sup>, Richmond, Indiana). Animals in this study were handled in accordance with the regulations in the ARVO Statement for the Use of Animals in Ophthalmic and Vision Research and the National Institutes of Health Guide for the Care and Use of Laboratory Animals. This study was approved by The University of Georgia Institutional Animal Care and Use Committee.

#### 2.2. Genotype confirmation

Tail biopsy samples from all WT and Sey mice were placed in individual tubes with tail lysis buffer (100mM Tris HCl pH 8.5, 5mM EDTA, 0.2% SDS, and 200mM NaCl) and 100μg Proteinase K/mL. Following complete lysis, the tubes were vortexed and centrifuged @ 13 600 rcf for 10 minutes. The supernatant was mixed with 500μL isopropanol to induce genomic DNA precipitation. After centrifugation (5 min. @ 11 333 rcf), the supernatant was removed and the DNA was allowed to dry briefly at RT.

The DNA was then dissolved in 100μL Tris EDTA (10mM Tris HCl, 1mM EDTA; pH 7.5) and incubated at 37°C overnight.

Genotyping was performed similar to a previously described method [23, 37]. Briefly, 3μL of genomic DNA was added to a 22μL mixture of dNTP (200 μM each dNTP, Fisher Scientific), PCR buffer with 1.5 mM Mg²+ (Roche Diagnostics), Pax6 forward (5' GAG GAA CCA GAG AAG ACA GGC 3') and reverse (5' GCA TAG GCA GGT TGT TTG CC 3') primer (0.2μM each), Taq DNA polymerase (1.25 U per reaction, Sigma), and molecular grade, distilled, and deionized water. For PCR, samples were placed in a PTC-100 Programmable Thermal Controller (MJ Research Inc.) for the following: 5min @ 95°C; 40 cycles of [1min. @ 95°C, 1min. @ 60°C, 2min. @ 72°C]; 7 min. @ 72°C. A 5μL mixture of 10x Buffer (Buffer 3; New England Biolabs) and HincII restriction enzyme (New England Biolabs) was added to the PCR sample and tubes were incubated at 37°C overnight. Ethidium bromide stained PCR products were fractionated on a 2% agarose gel.

## 2.3. In vivo corneal epithelial wounding

A pilot study using WT mice (n=21) was performed to develop the corneal wounding protocol. Ophthalmic examination of the WT mice using slit lamp biomicroscopy and fluorescein stain was normal. The mice were anesthetized with intraperitoneal ketamine hydrochloride (100mg/kg) and xylazine hydrochloride (10mg/kg). Wounding of the central cornea was performed in the left eye under 2.5x magnification by applying for 1 minute a sterile, 1.75mm disk of single-ply tissue (Kimwipe®) saturated in 2μL of n-heptanol [68, 73]. An identical procedure was repeated on the right eye using physiologic saline instead of n-heptanol. Buprenorphine

hydrochloride (0.05-0.01mg/kg SQ) was administered pre- and post-operatively every 6-12 hours as needed for analgesia. Mice were evaluated on days 1, 2, 4, 7, 14, and 28 post wounding. Ophthalmic examination included slit lamp biomicroscopy (SL-15; Kowa Optimed, Inc.; Torrance, CA), application of fluorescein stain (Fluor-I-Strip-A.T.; Bausch & Lomb Pharmaceuticals, Inc.; Tampa, FL) to identify the area of epithelial loss (ulcer), and digital photography (Nikon D-100; Melville, NY) of both eyes in all mice. A total of 3-5 randomly selected mice were euthanized (CO<sub>2</sub> and cervical dislocation) on each examination day.

In the wound healing comparison phase, WT (n=58) and Sey (n=40) mice were wounded using the protocol established in the pilot study, except no disk was applied to the right eye. To account for difference in corneal size between groups, a 1.75mm disk was used for WT and a 1.2mm disk for Sey. The 1.2mm diameter disk size was determined by comparing numerous disk sizes from 0.75 – 1.5mm and estimating the amount of cornea wounded for the average Sey cornea. The 1.2mm diameter disk was chosen as it most closely approximated the amount of cornea wounded for WT mice. Mice were evaluated on days 1, 2, 3 (if fluorescein positive on day 2), 4, 7, 14, and 28 post wounding. A total of 3-5 mice were euthanized (CO<sub>2</sub> and cervical dislocation) on each examination day.

#### 2.4. Comparison of corneal wound healing

Digital photographs of the cornea were taken immediately post wounding and fluorescein staining (WT=43; Sey=29). The total corneal area and the area of the corneal wound on day 0 was determined for each mouse by evaluation of digital photographs using image analysis software (ImageJ [74]) on a Power Macintosh G4 computer running

OSX (Fig. 1). The number of days to negative fluorescein staining (wound healing) was recorded for each mouse. Mice were examined as indicated above until complete corneal wound healing.

#### 2.5. Histology

Immediately after euthanasia, both eyes from each mouse (WT=79; Sey=40) were immersed in 4% paraformaldehyde and stored at 4°C. Globes were measured (Castroviejo calipers) at the horizontal equator using 2.5x magnification and then processed and embedded in paraffin wax. For routine microscopy, vertical sections one quarter of the way into the globe were made based on prior measurements. Four micron sections were then deparaffinized in two changes of xylene, rehydrated in graded ethanol (100%, 100%, 95%, 95%, and 70%), and rinsed in water. Application of Gill II Hematoxylin (Surgipath<sup>TM</sup>, Richmond, II.), 95% ethanol, and Eosin (Surgipath<sup>TM</sup>, Richmond, II.) was then followed by 4 changes of 100% ethanol, 1 change of acetone/xylene, and 3 changes of xylene. Samples were mounted on a slide and a coverslip applied using PermaMount (Vector Laboratories). Corneal morphology of non-wounded and wounded WT and Sey mice was described and compared.

## 2.6. Molecular Marker Analysis

Sections of each eye were deparaffinized, rehydrated, and incubated with 3% hydrogen peroxide for 5 minutes to quench endogenous peroxidase activity. The number of mice evaluated for p63 staining is as follows: day 1 WT/Sey = 3/4; day 2 WT/Sey = 4/4; day 4 WT/Sey = 8/5; day 28 WT/Sey = 7/4, respectively. For p63 immunostaining, monoclonal anti-p63 primary antibody derived from the 4A4 hybridoma in BALB/c mice raised against mouse  $\Delta$ Np63 (Sigma, St. Louis, MO; stock diluted 1:500) was used. As

the primary antibody was made in a mouse and being used on mouse tissue, a MOM kit (Vector Laboratories, Burlingame, CA) which is specifically designed to decrease background was used following manufacturer's directions. The primary antibody was applied for 30 minutes. The non-wounded corneas of WT (n=46) and Sey (n=24) mice were evaluated for expression of sVEGFR-1. For sVEGFR-1 immunostaining, Power Block<sup>TM</sup> Universal Blocking Reagent (BioGenex, San Ramon, CA) was applied for 5 minutes to block non-specific binding of antibody. Membrane bound VEGFR-1 antibody was used (R&D Systems, Minneapolis, MN; rat monoclonal; stock diluted 1:100). Samples were incubated with the primary antibody for 60 minutes, followed by 10 minutes with biotinylated anti-rat IgG (Vector Laboratories, Burlingame, CA) and 10 minutes with LSAB2 Streptavidin-HRP (Dako, Carpinteria, CA). For both immunostains, incubation with 3,3'-diaminobenzidine (DAB; Dako, Carpinteria, CA) was performed to localize peroxidase activity. A Dako Autostainer Plus Universal Staining System (Dako, Carpinteria, CA) was used for all immunostaining. Counterstaining with Gills II hematoxylin (Surgipath<sup>TM</sup>, Richmond, II.) was performed followed by graded ethanol dehydration (70%, 95%, 95%, 100%, 100%) and 2 changes of xylene. Sections were mounted on a slide and a coverslip applied. Positive controls (mouse kidney) for both antibodies were performed at the same time under the same conditions as the sample tissue. Two negative controls (PBS and normal mouse serum for p63; PBS and normal rat serum for sVEGFR-1) were performed by incubating the tissue (mouse kidney) with the negative control instead of the primary antibody under the same conditions.

For analysis of p63 expression, the corneal epithelium was divided into three sections. First, the limbal epithelium was identified based on its location adjacent to the

base of the iris, as well as cellular and underlying stromal morphology characterized by a thinner epithelial layer (2-4 cell layers thick) with a loose, well vascularized underlying stroma and lack of goblet cells [75, 76]. The peripheral and central regions were defined by counting the remaining basal epithelial cells and dividing in half. All basal epithelial cells from the limbal and peripheral regions were scored as either positive or negative. The central region was not counted due to wounding. The expression of sVEGFR-1 was scored as either positive or negative and anatomic localization was recorded.

#### 2.7. Statistical Analysis

All analyses were performed using SAS V 9.2 (Cary, NC). The proportion of the cornea wounded was compared between groups using a Student's t-test. The number of days to negative fluorescein staining was compared using the Chi-Square test. The number of p63 staining basal epithelial cells was recorded and compared between time points and groups for each section of cornea (limbal and peripheral) by ANOVA.

### 3. Results

#### 3.1. Ophthalmic examination and histopathologic findings

On evaluation prior to wounding, slit lamp biomicroscopy of the anterior segment of all WT mice was normal (Fig's. 2, 3a). Examination of Sey mice revealed variation in phenotype, however most expressed corneal opacity, neovascularization, iris hypoplasia, and anterior cortical cataract (Fig's. 2, 4a).

Histology of the non-wounded WT cornea (Fig. 3b) revealed a basal layer in which the epithelial cells varied in shape from cuboidal to short columnar to polygonal and contained dark to variably basophilic round to oval nuclei and lightly eosinophilic cytoplasm. As epithelial cells migrated superficially, nuclei became more oval and then

horizontally elongated, while the cytoplasm became more darkly eosinophilic. The epithelial layer was 5-7 cells thick centrally and 3-4 cells thick peripherally and did not rest upon a clearly defined basal lamina. The corneal stroma consisted of organized, tightly arranged collagen fibers. Evenly distributed within the collagen were keratocytes with fusiform to polygonal cell nuclei and indistinct cell borders. The endothelial layer consisted of a single layer of cuboidal shaped cells with basophilic nuclei and a clear vacuolated to eosinophilic cytoplasm. Separating the endothelial layer and the deep stroma was a faint, deeply eosinophilic, hyaline membrane (Descemet's membrane).

Comparatively, histopathology of the non-wounded Sey cornea was markedly different (Fig. 4). The central epithelium was typically only 3-4 cells (rarely 1-2) thick while the periphery was usually 1-3 cells thick. The epithelial layer of most Sey mice (31/39) contained a variable number of epithelial cells with a large, lightly basophilic cytoplasmic vacuole. These vacuoles were consistent with mucin on H&E and this was confirmed with PAS staining (Fig. 5). The cuboidal basal epithelial cells contained basophilic nuclei in which the chromatin was intermittently dispersed and a lightly eosinophilic cytoplasm with tiny clear vacuoles. There was no discernible underlying basal lamina even with PAS staining. The more superficial epithelial cells had nuclei that were more basophilic and cigar shaped with a more hypereosinophilic cytoplasm. In general, the corneal (stromal) thickness in the Sey was greater than that of WT. The anterior stroma typically contained densely packed and disorganized collagenous lamella. The amount of collagenous stroma appears to be increased over that seen in the WT. In all samples with sufficient cornea for evaluation, the peripheral to mid anterior stroma contained small caliber blood vessels (39/39). Associated with the vascularization was

mild to moderate corneal edema. Additional histopathologic findings included iris hypoplasia (Fig's. 6, 7), anterior cortical cataract (Fig. 8), and anterior lens dislocation (Fig. 9). All Sey had iris hypoplasia of varying degrees. While anterior cortical cataract was present in some mice, accurate quantification of the actual number with this lesion was difficult due to the relatively small size of the lesion. A single mouse had lens dislocation.

Corneal wounding with n-heptanol removed the epithelial layer in all mice (Fig. 10). Corneal histopathology post wounding in both groups was similar with a few minor differences. In addition to those findings previously described in non wounded corneas, there was mild to moderate, anterior stromal, purulent keratitis characterized by infiltrations of neutrophils with rare lymphocytes and plasma cells. Anterior stromal neovascularization and focal superficial ulceration was present in eyes that were fluorescein positive at enucleation. In some cases, there appeared to be a more prominent inflammatory cell response in the corneal stroma of Sey mice (Fig. 11), however overall the variation in inflammatory cell infiltrate did not appear to differ dramatically enough to adequately quantify.

Typical findings in ulcerated areas of both wounded WT and Sey eyes included a focal area of stroma that was devoid of an overlying epithelial layer. The epithelium adjacent to the ulcer was usually one cell layer thick and progressively increased in cell thickness further from the ulcerated site. Many of the basal epithelial cells adjacent to the ulcer and at the limbus contained clear cytoplasmic vacuoles, consistent with intracellular edema. The mid to anterior corneal stroma contained an infiltration of blood vessels and

mature neutrophils. There was no difference in the number of goblet cells in wounded vs. non-wounded Sey corneas.

#### 3.2. In vivo corneal wound healing

The genotype for all mice was confirmed (Fig. 12). The pilot study allowed time to perfect the wounding technique. All left eyes revealed axial corneal ulceration (n=21). A single right eye sustained a pinpoint paraxial ulcer that healed uneventfully by the next day's examination. In the comparison phase, the proportion of cornea wounded between WT and Sey mice was not significantly different (WT=56.3% +/- 13.5% vs. Sey=52.0% +/- 12.2%; p=0.1585). Time to corneal wound healing is summarized in Fig. 13. The wounded cornea of all mice was fluorescein positive on day 0. On days 1 and 4, there was no significant difference in number of mice that were fluorescein positive (p=0.2201). However, the proportion of eyes that were fluorescein positive was significantly higher in the Sey group than the WT group on days 2 (p=0.0187) and 3 (p=0.0312). All corneal ulcers were completely healed (fluorescein negative) by day 7. 3.3. Expression of p63 and sVEGFR-1

All samples were strongly positive for p63 in the nuclei of limbal and peripheral basal corneal epithelium. Statistical evaluation revealed no significant difference in basal epithelial p63 expression between WT and Sey mice or time points for any section of cornea for either eye (p>0.05). There was no staining within the more superficial epithelium or corneal stroma (Fig's. 14-20) in all WT and most Sey. Occasionally, Sey mice (29%) had epithelial nuclei superficial to the basal layer which stained positive for p63.

Expression of sVEGFR-1 in the cornea was comparable in all WT and Sey mice (Fig's. 21-25). In both non-wounded groups there was prominent basal staining within the perilimbal cornea localizing most prominently within the cytoplasm of stromal keratocytes and endothelium (posterior epithelium) and within the extracellular space of the associated corneal stroma. Rarely, there was light staining within the cytoplasm of adjacent epithelial (anterior) cells. In WT mice, the central cornea was devoid of staining (Fig 26). However, in the Sey group, a total of 8 (33%) mice had central to peripheral corneal staining (Fig 27).

#### 4. Discussion

## 4.1. Anterior segment evaluation

Ophthalmic examination using a slit lamp biomicroscope allows for thorough analysis of the anterior segment. These findings are helpful in correlating observed gross changes with microscopic pathology. This is the first detailed slit lamp examination of Sey<sup>Neu</sup> mice performed to indicate the prevalence of specific anterior segment pathology. Corneal opacity was common and associated with vascularization. Interestingly, while corneal vascularization was clinically detected in only 50% (20/40) of Sey mice at initial exam, histopathologically 100% (39/39) of the examined corneas were vascularized. This is likely secondary to the very fine, small caliber vessels in some mice and indicates an underlying disturbance in the mechanism(s) responsible for maintenance of corneal avascularity even in grossly avascular eyes. The relatively thin corneal epithelial layer, dense and disorganized stromal collagen, and basophilic cytoplasmic vacuole within the epithelial cells (PAS positive goblet cell) are similar to previous findings [53]. The thin epithelial layer has been suggested to be secondary to increased shearing of squamous

cells from the corneal surface due to impaired cytokeratin expression. This morphology may also be secondary to decreased levels of Pax6 resulting in abnormal epithelial development [48]. The increased corneal thickness in Sey is likely secondary to stromal edema, neovascularization and increased collagen production, however the underlying mechanism of this pathology is not understood. Iris hypoplasia was identified with biomicroscopy and confirmed with histopathology.

While there is variation in the severity of cataract and portion of lens affected, the anterior cortical cataract observed clinically appears microscopically as an accumulation of disorganized and proliferating anterior lens epithelial cells with an intact overlying lens capsule. The disorganized anterior epithelial cells appear to be secreting a PAS positive material (Fig 8b). This may represent a continued attempt at lens capsule production. Given the gross and microscopic findings, this pathology may represent a defective detachment of the lens vesicle from the overlying surface ectoderm during development. To the authors' knowledge, this cataract has not been described in the Sey mouse.

A single Sey mouse expressed unique lenticular pathology (Fig. 9). Clinically, the lens was within the anterior chamber and there was corneal opacity which was most prominent centrally. Microscopically, there was a relative thickening and fibrovascular pannus with edema associated with the central corneal stroma. The anterior lens capsule was complete and in contact with the posterior cornea. There was disorganization and proliferation of the anterior lens epithelium similar to cataractous changes in other Sey mice. One potential mechanism for this pathology is incomplete separation during embryology, as suggested above. Alternatively, this may represent an anterior lens

luxation secondary to hypoplasia of the anterior uvea (ciliary body and lens) and malformation of the suspensory apparatus (zonules) necessary for maintaining the lens in normal anatomic position. Further study to characterize the lens and anterior uvea / zonules will be important in understanding the lenticular pathology inherent to Pax6 deficiency.

Finally, there was an increase in inflammatory cell infiltrate in the wounded Sey eyes compared to the WT eyes at the same time post wounding. This has been previously reported [70]. This phenomenon may be secondary to an increased stimulus for infiltration or a perturbation of mechanisms inherent to its regulation.

## 4.2. In vivo corneal wound healing

In vivo corneal wounding with n-heptanol as described was a valid technique to provide evaluation of wound healing ability in the mice of this study. The corneal epithelium was consistently removed without histopathologic evidence of stromal loss. Options for corneal wounding are numerous and include n-heptanol, sodium hydroxide, and mechanical removal. Sodium hydroxide can induce dramatic anterior uveitis (including hyphema and hypopyon) in the murine species [77]. Mechanical removal, even under an operating microscope, has been shown to be inaccurate and imprecise in the rabbit model [73]. Thus, in the significantly smaller eye of the mouse, it is not reasonable to assume that the amount of cornea wounded by mechanical removal will be consistent enough for valid comparisons of wound healing rates. Application of n-heptanol has been shown to be a fast, accurate, and reproducible technique for consistent removal of corneal epithelium [73]. The vast majority of mice in this study did not exhibit outward signs of pain (blepharospasm, epiphora, rubbing, or withdrawal from the

group) the day after wounding and there was no clinical or histologic evidence of infectious keratitis. Topical ophthalmic anti-inflammatory or antibiotic medication was not used in this study due to their potential to inhibit wound healing [78, 79]. This would have complicated interpretation of wound healing data.

In the *in vivo* corneal wounding model reported here, Sey mice exhibited a statistically significant delay in corneal healing compared to WT mice at days 2 and 3 post wounding. This delay may in part be secondary to depletion in the cellular machinery required for wound healing or a deficiency in limbal stem cells. Overall, the difference between wounding times were not as dramatic as expected. The majority of WT and Sey mice healed within the first 48 hours, which suggests that there is not a dramatic difference in wound healing ability between these two groups of mice after a single wounding. This would be consistent with the progressive corneal pathology in humans with ARK and Sey mice from the cumulative effects of a Pax6 deficiency over time. Chronic corneal microtrauma or ulceration with concomitant abnormal healing in Pax6 deficient humans and mice may lead to epithelial and stromal opacity. This wounding model provides a baseline to further study the pathophysiology of ARK.

## 4.3. Evaluation of limbal progenitor cells

In this study we evaluated p63, a marker of the proliferative cell pool of the corneal epithelium, to determine if these cells, in an *in vivo* model of corneal wounding, are depleted or become depleted over time. The corneal epithelial stem cells are widely accepted to reside within the basal layer of the corneoscleral limbus. Support for this location is based on its unique presence of slow-cycling cells (label-retaining cells) [75, 76, 80-82], primitive differentiation compared to the rest of the cornea [83-89], capacity

for unlimited self renewal [90, 91], high proliferative potential after activation by wounding [75, 92, 93], morphologic criteria [94], and abnormal corneal wound repair after removal of the limbal epithelium [95-97]. To date, a cell marker has not been discovered that definitively labels corneal stem cells. This study revealed no significant difference in p63 expression in the basal layer of the corneal epithelium of either eye between WT and Sey mice at any time point before or after wounding. These findings suggest that the delay in corneal healing does not appear to be due to depletion in p63 cellular expression over time, which is consistent with previous studies [48]. Expression of p63 within the nuclei of epithelial cells superficial to the basal layer in Sey mice may indicate defective cell fate decision making. Identification of specific markers for corneal epithelial stem cells in addition to assessing the function of these cells will allow for a better assessment of this cell population in ARK. It is possible that a model which induces multiple woundings (chronic wound model) would identify a deficiency in the proliferative cell pool over time in Sey mice. The results reported in this study support a combination of underlying wound healing deficiency and inherent abnormal epithelial differentiation and stromal changes as the underlying etiology of ARK, rather than overall depletion in limbal stem cells.

## 4.4 Localization of sVEGFR-1 in WT and Sey mice cornea

One of the most prominent manifestations of ARK is widespread corneal vascularization [38, 39], a change which significantly compromises vision. The unique quality of corneal avascularity is crucial in maintaining a clear visual axis. Vascular endothelial growth factor (VEGF)-A is a potent stimulator of angiogenesis in numerous tissues and is expressed in the cornea [98]. A soluble factor which binds VEGF-A with

high affinity (sVEGFR-1) and inhibits its activity has been identified and suggested to play a role in maintaining corneal avascularity [99]. Inhibition of VEGF-A with sVEGFR-1 reduces corneal vascularization [51, 100]. A more recent study in mice shows inhibition of corneal sVEGFR-1 with an antagonist resulted in corneal vascularization [101]. sVEGFR-1 is reported to be deficient in Pax6<sup>+/-</sup> mice [50].

A commercially available sVEGFR-1 antibody is not available; therefore, membrane bound VEGFR-1 antibody was used. This antibody detects both the soluble and membrane bound protein (extracellular domain). Previous work has shown the membrane bound form to be absent in murine cornea, and thus positive staining using this antibody should identify sVEGFR-1 [50]. In this study, we have shown for the first time comparable immunolocalization of sVEGFR-1 in the cornea of WT and Sey mice. Given that corneal vascularization initiates from the limbus, the prominence of perilimbal staining in this study is suggestive of a role for this protein in the maintenance of an avascular cornea. In a recent study of sVEGFR-1 in the cornea, there was no detectable basal level of sVEGFR-1 within the corneal epithelial cells, while it was constitutively secreted within stromal fibroblasts [102]. These findings are consistent with the localization of sVEGFR-1 in this study.

Given the previous study of sVEGFR-1 in Sey mice [50], these were unexpected findings. One explanation may be the use of different Sey strains, however the strain used in the previous report was not indicated. There are numerous mice with various mutations in the Pax6 gene which result in varying phenotypic expression and genetic modifier effects. Immunohistochemical analysis is, inherently, qualitative and thus further quantitative work (western blot) is required to determine specific levels of this

protein in the cornea of these mice. This investigation is underway. Regardless, the comparable expression of sVEGFR-1 in mice with avascular (WT) and vascular (Sey) corneal phenotypes reported here suggests that it alone is likely not responsible for the corneal vascularization present in Sey mice.

### 5. References

- 1. Graw, J., Genetic aspects of embryonic eye development in vertebrates. Dev Genet, 1996. **18**(3): p. 181-97.
- 2. Dahl, E., H. Koseki, and R. Balling, *Pax genes and organogenesis*. Bioessays, 1997. **19**(9): p. 755-65.
- 3. Ashery-Padan, R., et al., Pax6 activity in the lens primordium is required for lens formation and for correct placement of a single retina in the eye. Genes Dev, 2000. **14**(21): p. 2701-11.
- 4. Azuma, N., et al., *Mutations of the PAX6 gene detected in patients with a variety of optic-nerve malformations.* Am J Hum Genet, 2003. **72**(6): p. 1565-70.
- 5. Collinson, J.M., R.E. Hill, and J.D. West, *Analysis of mouse eye development with chimeras and mosaics*. Int J Dev Biol, 2004b. **48**(8-9): p. 793-804.
- 6. Davis, J., et al., Requirement for Pax6 in corneal morphogenesis: a role in adhesion. J Cell Sci, 2003. **116**(Pt 11): p. 2157-67.
- 7. Davis-Silberman, N., et al., *Genetic dissection of Pax6 dosage requirements in the developing mouse eye.* Hum Mol Genet, 2005. **14**(15): p. 2265-76.

- 8. Kanakubo, S., et al., Abnormal migration and distribution of neural crest cells in Pax6 heterozygous mutant eye, a model for human eye diseases. Genes Cells, 2006. 11(8): p. 919-33.
- 9. Mathers, P.H. and M. Jamrich, *Regulation of eye formation by the Rx and pax6 homeobox genes*. Cell Mol Life Sci, 2000. **57**(2): p. 186-94.
- 10. Nishina, S., et al., *PAX6 expression in the developing human eye*. Br J Ophthalmol, 1999. **83**(6): p. 723-7.
- 11. Tzoulaki, I., I.M. White, and I.M. Hanson, *PAX6 mutations: genotype-phenotype correlations*. BMC Genet, 2005. **6**(1): p. 27.
- 12. Halder, G., P. Callaerts, and W.J. Gehring, *New perspectives on eye evolution*.

  Curr Opin Genet Dev, 1995b. **5**(5): p. 602-9.
- 13. Halder, G., P. Callaerts, and W.J. Gehring, *Induction of ectopic eyes by targeted expression of the eyeless gene in Drosophila*. Science, 1995a. **267**(5205): p. 1788-92.
- 14. Kozmik, Z., The role of Pax genes in eye evolution. Brain Res Bull, 2008. 75(2-4): p. 335-9.
- Reza, H.M., Y. Takahashi, and K. Yasuda, Stage-dependent expression of Pax6 in optic vesicle/cup regulates patterning genes through signaling molecules.
   Differentiation, 2007. 75(8): p. 726-36.
- 16. Favor, J., et al., Relationship of Pax6 activity levels to the extent of eye development in the mouse, Mus musculus. Genetics, 2008. **179**(3): p. 1345-55.

- 17. Gehring, W.J., *The master control gene for morphogenesis and evolution of the eye.* Genes Cells, 1996. **1**(1): p. 11-5.
- 18. Gehring, W.J., New perspectives on eye development and the evolution of eyes and photoreceptors. J Hered, 2005. **96**(3): p. 171-84.
- 19. Hogan, B.L., et al., Small eyes (Sey): a homozygous lethal mutation on chromosome 2 which affects the differentiation of both lens and nasal placodes in the mouse. J Embryol Exp Morphol, 1986. **97**: p. 95-110.
- 20. Glaser, T., J. Lane, and D. Housman, *A mouse model of the aniridia-Wilms tumor deletion syndrome*. Science, 1990. **250**(4982): p. 823-7.
- 21. van der Meer-de Jong, R., et al., Location of the gene involving the small eye mutation on mouse chromosome 2 suggests homology with human aniridia 2 (AN2). Genomics, 1990. **7**(2): p. 270-5.
- 22. Ton, C.C., et al., *Positional cloning and characterization of a paired box- and homeobox-containing gene from the aniridia region*. Cell, 1991. **67**(6): p. 1059-74.
- 23. Hill, R.E., et al., Mouse small eye results from mutations in a paired-like homeobox-containing gene. Nature, 1991. **354**(6354): p. 522-5.
- 24. Ton, C.C., H. Miwa, and G.F. Saunders, *Small eye (Sey): cloning and characterization of the murine homolog of the human aniridia gene*. Genomics, 1992. **13**(2): p. 251-6.

- 25. Hill, R.E., et al., Mouse Small eye results from mutations in a paired-like homeobox-containing gene. Nature, 1992. **355**(6362): p. 750.
- 26. Quinn, J.C., J.D. West, and R.E. Hill, *Multiple functions for Pax6 in mouse eye* and nasal development. Genes Dev, 1996. **10**(4): p. 435-46.
- 27. Collinson, J.M., et al., *Primary defects in the lens underlie complex anterior* segment abnormalities of the Pax6 heterozygous eye. Proc Natl Acad Sci U S A, 2001. **98**(17): p. 9688-93.
- 28. Ziman, M.R., et al., Pax genes in development and maturation of the vertebrate visual system: implications for optic nerve regeneration. Histol Histopathol, 2001.

  16(1): p. 239-49.
- 29. Zhang, W., et al., Quantitation of PAX6 and PAX6(5a) transcript levels in adult human lens, cornea, and monkey retina. Mol Vis, 2001. 7: p. 1-5.
- 30. Ashery-Padan, R. and P. Gruss, *Pax6 lights-up the way for eye development*. Curr Opin Cell Biol, 2001. **13**(6): p. 706-14.
- 31. Simpson, T.I. and D.J. Price, *Pax6; a pleiotropic player in development.*Bioessays, 2002. **24**(11): p. 1041-51.
- 32. Pichaud, F. and C. Desplan, *Pax genes and eye organogenesis*. Curr Opin Genet Dev, 2002. **12**(4): p. 430-4.
- 33. Collinson, J.M., et al., *The roles of Pax6 in the cornea, retina, and olfactory epithelium of the developing mouse embryo.* Dev Biol, 2003. **255**(2): p. 303-12.

- 34. Hanson, I.M., *PAX6 and congenital eye malformations*. Pediatr Res, 2003. **54**(6): p. 791-6.
- 35. Ramaesh, K., et al., Evolving concepts on the pathogenic mechanisms of aniridia related keratopathy. Int J Biochem Cell Biol, 2005a. **37**(3): p. 547-57.
- 36. Koroma, B.M., J.M. Yang, and O.H. Sundin, *The Pax-6 homeobox gene is*expressed throughout the corneal and conjunctival epithelia. Invest Ophthalmol

  Vis Sci, 1997. **38**(1): p. 108-20.
- 37. Kim, J. and J.D. Lauderdale, *Analysis of Pax6 expression using a BAC transgene reveals the presence of a paired-less isoform of Pax6 in the eye and olfactory bulb.* Dev Biol, 2006. **292**(2): p. 486-505.
- 38. Margo, C.E., Congenital aniridia: a histopathologic study of the anterior segment in children. J Pediatr Ophthalmol Strabismus, 1983. **20**(5): p. 192-8.
- 39. Nelson, L.B., et al., *Aniridia. A review*. Surv Ophthalmol, 1984. **28**(6): p. 621-42.
- 40. Khaw, P.T., *Aniridia*. J Glaucoma, 2002. **11**(2): p. 164-8.
- 41. Walton, D.S., *Aniridia (PAX6(+/-))*. J Pediatr Ophthalmol Strabismus, 2005. **42**(2): p. 128.
- 42. Mackman, G., F.S. Brightbill, and J.M. Optiz, *Corneal changes in aniridia*. Am J Ophthalmol, 1979. **87**(4): p. 497-502.
- 43. Puangsricharern, V. and S.C. Tseng, *Cytologic evidence of corneal diseases with limbal stem cell deficiency*. Ophthalmology, 1995. **102**(10): p. 1476-85.

- 44. Nishida, K., et al., *Ocular surface abnormalities in aniridia*. Am J Ophthalmol, 1995. **120**(3): p. 368-75.
- 45. Dua, H.S. and A. Azuara-Blanco, *Limbal stem cells of the corneal epithelium*. Surv Ophthalmol, 2000. **44**(5): p. 415-25.
- 46. Holland, E.J., A.R. Djalilian, and G.S. Schwartz, *Management of aniridic keratopathy with keratolimbal allograft: a limbal stem cell transplantation technique*. Ophthalmology, 2003. **110**(1): p. 125-30.
- 47. Collinson, J.M., et al., Corneal development, limbal stem cell function, and corneal epithelial cell migration in the Pax6(+/-) mouse. Invest Ophthalmol Vis Sci, 2004a. **45**(4): p. 1101-8.
- 48. Ramaesh, T., et al., *Developmental and cellular factors underlying corneal epithelial dysgenesis in the Pax6+/- mouse model of aniridia.* Exp Eye Res, 2005b. **81**(2): p. 224-35.
- 49. Ambati, B.K., et al., *Soluble vascular endothelial growth factor receptor-1* contributes to the corneal anti-angiogenic barrier. Br J Ophthalmol, 2006b.
- 50. Ambati, B.K., et al., *Corneal avascularity is due to soluble VEGF receptor-1*.

  Nature, 2006a. **443**(7114): p. 993-7.
- 51. Lai, C.M., et al., *Inhibition of angiogenesis by adenovirus-mediated sFlt-1*expression in a rat model of corneal neovascularization. Hum Gene Ther, 2001.

  12(10): p. 1299-310.

- 52. Liu, J.J., W.W. Kao, and S.E. Wilson, *Corneal epithelium-specific mouse keratin K12 promoter*. Exp Eye Res, 1999. **68**(3): p. 295-301.
- 53. Ramaesh, T., et al., *Corneal abnormalities in Pax6+/- small eye mice mimic human aniridia-related keratopathy*. Invest Ophthalmol Vis Sci, 2003. **44**(5): p. 1871-8.
- 54. Shiraishi, A., et al., *Identification of the cornea-specific keratin 12 promoter by in vivo particle-mediated gene transfer*. Invest Ophthalmol Vis Sci, 1998. **39**(13): p. 2554-61.
- 55. Kucerova, R., et al., *Cell surface glycoconjugate abnormalities and corneal epithelial wound healing in the pax6+/- mouse model of aniridia-related keratopathy.* Invest Ophthalmol Vis Sci, 2006. **47**(12): p. 5276-82.
- 56. Leiper, L.J., et al., *The roles of calcium signaling and ERK1/2 phosphorylation in a Pax6+/- mouse model of epithelial wound-healing delay.* BMC Biol, 2006. **4**: p. 27.
- 57. Sivak, J.M., et al., Pax-6 expression and activity are induced in the reepithelializing cornea and control activity of the transcriptional promoter for matrix metalloproteinase gelatinase B. Dev Biol, 2000. 222(1): p. 41-54.
- 58. Jastaneiah, S. and A.A. Al-Rajhi, *Association of aniridia and dry eyes*.

  Ophthalmology, 2005. **112**(9): p. 1535-40.
- 59. Ou, J., et al., *Chronic wound state exacerbated by oxidative stress in Pax6+/-aniridia-related keratopathy*. J Pathol, 2008. **215**(4): p. 421-30.

- 60. Leiper, L.J., et al., *Control of patterns of corneal innervation by Pax6*. Invest Ophthalmol Vis Sci, 2009. **50**(3): p. 1122-8.
- 61. Tiller, A.M., et al., *The influence of keratoplasty on visual prognosis in aniridia: a historical review of one large family.* Cornea, 2003. **22**(2): p. 105-10.
- 62. Gomes, J.A., et al., *Recurrent keratopathy after penetrating keratoplasty for aniridia*. Cornea, 1996. **15**(5): p. 457-62.
- 63. Kremer, I., et al., *Results of penetrating keratoplasty in aniridia*. Am J Ophthalmol, 1993. **115**(3): p. 317-20.
- 64. Lopez-Garcia, J.S., et al., *Congenital aniridia keratopathy treatment*. Arch Soc Esp Oftalmol, 2006. **81**(8): p. 435-44.
- 65. Ozbek, Z. and I.M. Raber, Successful management of aniridic ocular surface disease with long-term bandage contact lens wear. Cornea, 2006. **25**(2): p. 245-7.
- 66. Rivas, L., et al., [Impression cytology study of dry eyes in patients with congenital aniridia]. Arch Soc Esp Oftalmol, 2003. **78**(11): p. 615-22.
- 67. Ueno, H., et al., Experimental transplantation of corneal epithelium-like cells induced by Pax6 gene transfection of mouse embryonic stem cells. Cornea, 2007. **26**(10): p. 1220-7.
- 68. Homma, R., et al., Induction of epithelial progenitors in vitro from mouse embryonic stem cells and application for reconstruction of damaged cornea in mice. Invest Ophthalmol Vis Sci, 2004. **45**(12): p. 4320-6.

- 69. Ramaesh, T., et al., *Increased apoptosis and abnormal wound-healing responses* in the heterozygous Pax6+/- mouse cornea. Invest Ophthalmol Vis Sci, 2006.

  47(5): p. 1911-7.
- 70. Sivak, J.M., et al., Transcription Factors Pax6 and AP-2alpha Interact To Coordinate Corneal Epithelial Repair by Controlling Expression of Matrix Metalloproteinase Gelatinase B. Mol Cell Biol, 2004. **24**(1): p. 245-57.
- 71. Lemp, M.A., Baudouin, C., Baum, J., Dogru, M., Foulks, G.N., Kinoshita, S., Laibson, P., and J. McCulley, Murube, J., Pflugfelder, S.C., Roloando, M., Toda, I., The definition and classification of dry eye disease: report of the Definition and Classification Subcommittee of the International Dry Eye WorkShop (2007). Ocul Surf, 2007. 5(2): p. 75-92.
- 72. Rolando, M. and M. Zierhut, *The ocular surface and tear film and their dysfunction in dry eye disease*. Surv Ophthalmol, 2001. **45 Suppl 2**: p. S203-10.
- 73. Cintron C, et al., A simple method for the removal of rabbit corneal epithelium utilizing n-heptanol. Ophthalmic Res., 1979(11): p. 90-96.
- 74. Rasband, W.S., *ImageJ*, U. S. National Institutes of Health, Bethesda, Maryland, USA, <a href="http://rsb.info.nih.gov/ij/">http://rsb.info.nih.gov/ij/</a>, 1997-2008. 1997-2008.
- 75. Cotsarelis, G., et al., Existence of slow-cycling limbal epithelial basal cells that can be preferentially stimulated to proliferate: implications on epithelial stem cells. Cell, 1989. 57(2): p. 201-9.

- 76. Lavker, R.M., et al., Relative proliferative rates of limbal and corneal epithelia.
  Implications of corneal epithelial migration, circadian rhythm, and suprabasally located DNA-synthesizing keratinocytes. Invest Ophthalmol Vis Sci, 1991. 32(6):
  p. 1864-75.
- 77. Sosne, G., et al., *Thymosin-beta4 modulates corneal matrix metalloproteinase levels and polymorphonuclear cell infiltration after alkali injury.* Invest Ophthalmol Vis Sci, 2005. **46**(7): p. 2388-95.
- 78. Hendrix, D.V., D.A. Ward, and M.A. Barnhill, Effects of antibiotics on morphologic characteristics and migration of canine corneal epithelial cells in tissue culture. Am J Vet Res, 2001. **62**(10): p. 1664-9.
- 79. Hendrix, D.V., D.A. Ward, and M.A. Barnhill, *Effects of anti-inflammatory drugs* and preservatives on morphologic characteristics and migration of canine corneal epithelial cells in tissue culture. Vet Ophthalmol, 2002. **5**(2): p. 127-35.
- 80. Bickenbach, J.R., *Identification and behavior of label-retaining cells in oral mucosa and skin.* J Dent Res, 1981. **60 Spec No C**: p. 1611-20.
- 81. Lehrer, M.S., T.T. Sun, and R.M. Lavker, *Strategies of epithelial repair:*modulation of stem cell and transit amplifying cell proliferation. J Cell Sci, 1998.

  111 (Pt 19): p. 2867-75.
- 82. Tseng, S.C. and S.H. Zhang, *Limbal epithelium is more resistant to 5-fluorouracil toxicity than corneal epithelium*. Cornea, 1995. **14**(4): p. 394-401.

- 83. Abe, K., et al., Establishment of an efficient BAC transgenesis protocol and its application to functional characterization of the mouse Brachyury locus. Exp Anim, 2004. **53**(4): p. 311-20.
- Kiritoshi, A., N. SundarRaj, and R.A. Thoft, *Differentiation in cultured limbal epithelium as defined by keratin expression*. Invest Ophthalmol Vis Sci, 1991.
  32(12): p. 3073-7.
- Kurpakus, M.A., M.T. Maniaci, and M. Esco, Expression of keratins K12, K4 and K14 during development of ocular surface epithelium. Curr Eye Res, 1994.
  13(11): p. 805-14.
- 86. Kurpakus, M.A., E.L. Stock, and J.C. Jones, *Expression of the 55-kD/64-kD* corneal keratins in ocular surface epithelium. Invest Ophthalmol Vis Sci, 1990. **31**(3): p. 448-56.
- 87. Liu, C.Y., et al., *Cornea-specific expression of K12 keratin during mouse development*. Curr Eye Res, 1993. **12**(11): p. 963-74.
- 88. Matic, M., et al., *Stem cells of the corneal epithelium lack connexins and metabolite transfer capacity.* Differentiation, 1997. **61**(4): p. 251-60.
- 89. Schermer, A., S. Galvin, and T.T. Sun, Differentiation-related expression of a major 64K corneal keratin in vivo and in culture suggests limbal location of corneal epithelial stem cells. J Cell Biol, 1986. **103**(1): p. 49-62.
- 90. Lindberg, K., et al., *In vitro propagation of human ocular surface epithelial cells for transplantation*. Invest Ophthalmol Vis Sci, 1993. **34**(9): p. 2672-9.

- 91. Pellegrini, G., et al., Location and clonal analysis of stem cells and their differentiated progeny in the human ocular surface. J Cell Biol, 1999. **145**(4): p. 769-82.
- 92. Ebato, B., J. Friend, and R.A. Thoft, *Comparison of limbal and peripheral human corneal epithelium in tissue culture*. Invest Ophthalmol Vis Sci, 1988. **29**(10): p. 1533-7.
- 93. Hernandez Galindo, E.E., et al., *Expression of Delta Np63 in response to phorbol* ester in human limbal epithelial cells expanded on intact human amniotic membrane. Invest Ophthalmol Vis Sci, 2003. **44**(7): p. 2959-65.
- 94. Romano, A.C., et al., Different cell sizes in human limbal and central corneal basal epithelia measured by confocal microscopy and flow cytometry. Invest Ophthalmol Vis Sci, 2003. **44**(12): p. 5125-9.
- 95. Chen, J.J. and S.C. Tseng, *Corneal epithelial wound healing in partial limbal deficiency*. Invest Ophthalmol Vis Sci, 1990. **31**(7): p. 1301-14.
- 96. Chen, J.J. and S.C. Tseng, *Abnormal corneal epithelial wound healing in partial-thickness removal of limbal epithelium*. Invest Ophthalmol Vis Sci, 1991. **32**(8): p. 2219-33.
- 97. Huang, A.J. and S.C. Tseng, *Corneal epithelial wound healing in the absence of limbal epithelium*. Invest Ophthalmol Vis Sci, 1991. **32**(1): p. 96-105.
- 98. Chang, J.H., et al., *Corneal neovascularization*. Curr Opin Ophthalmol, 2001. **12**(4): p. 242-9.

- 99. Kendall, R.L. and K.A. Thomas, *Inhibition of vascular endothelial cell growth*factor activity by an endogenously encoded soluble receptor. Proc Natl Acad Sci
  U S A, 1993. **90**(22): p. 10705-9.
- 100. Lai, C.M., et al., *Inhibition of corneal neovascularization by recombinant* adenovirus mediated antisense VEGF RNA. Exp Eye Res, 2002. **75**(6): p. 625-34.
- 101. Ponticelli, S., et al., *Modulation of angiogenesis by a tetrameric tripeptide that antagonizes vascular endothelial growth factor receptor 1.* J Biol Chem, 2008. **283**(49): p. 34250-9.
- 102. Kommineni, V.K., et al., *IFN-gamma acts as anti-angiogenic cytokine in the human cornea by regulating the expression of VEGF-A and sVEGF-R1*. Biochem Biophys Res Commun, 2008. **374**(3): p. 479-84.

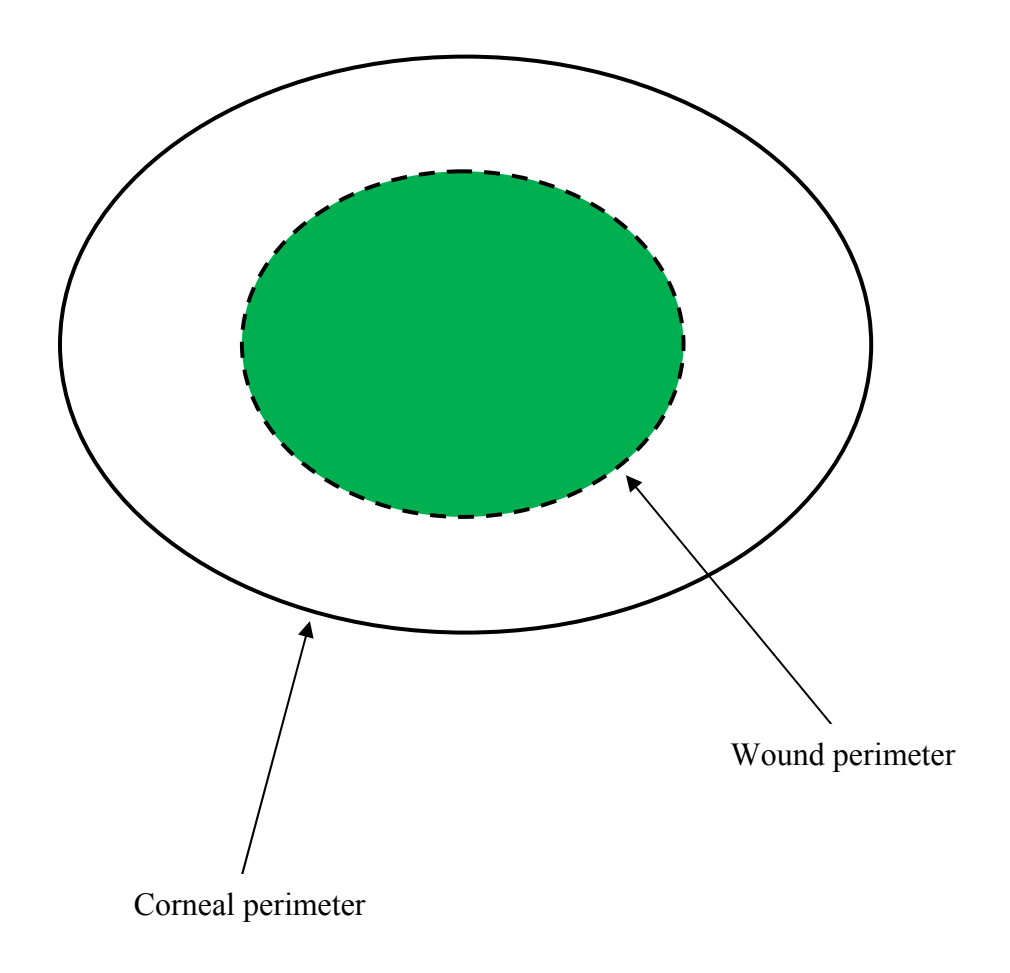


Figure 1: Schematic drawing showing method to determine total corneal size and wound (ulcer) size in WT and Sey mice. Using Image J software, corneal (continuous line) and wound (dotted line) perimeter were outlined. The proportion of wound area to total corneal area was determined for each mouse and compared between groups.

Pathology	Total
Microophthalmia	39/40
Iris hypoplasia	36/40
Corneal opacity	35/40
Cataract	27/40
Corneal vascularization	20/40
Keratolenticular adhesions	8/40
Lens luxation	1/40
Normal	0/40

Figure 2: Sey mice anterior segment slit lamp biomicroscopic examination findings. All WT mice ophthalmic examinations were normal.

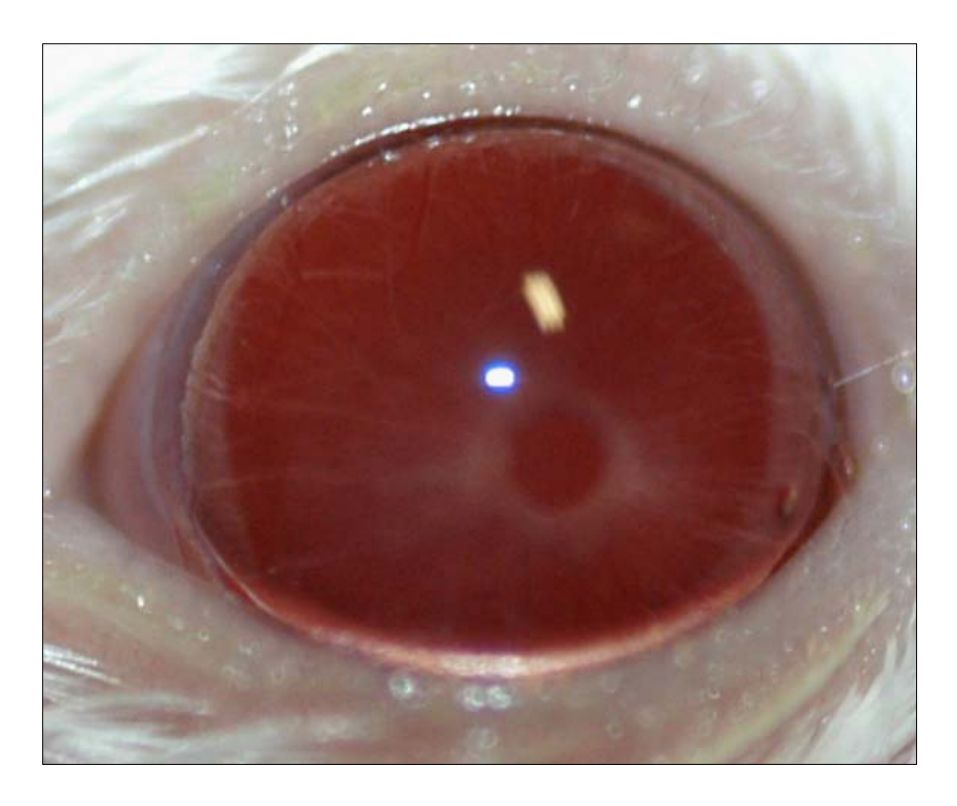




Figure 3: Representative clinical photograph (a) and corneal photomicrograph (b) of WT mouse prior to wounding. In the clinical photograph, note the normal ocular shape and clear cornea. Microscopically, the cornea was characterized by a stratified, squamous epithelial layer 5-7 cells thick and an organized underlying collagenous stroma.

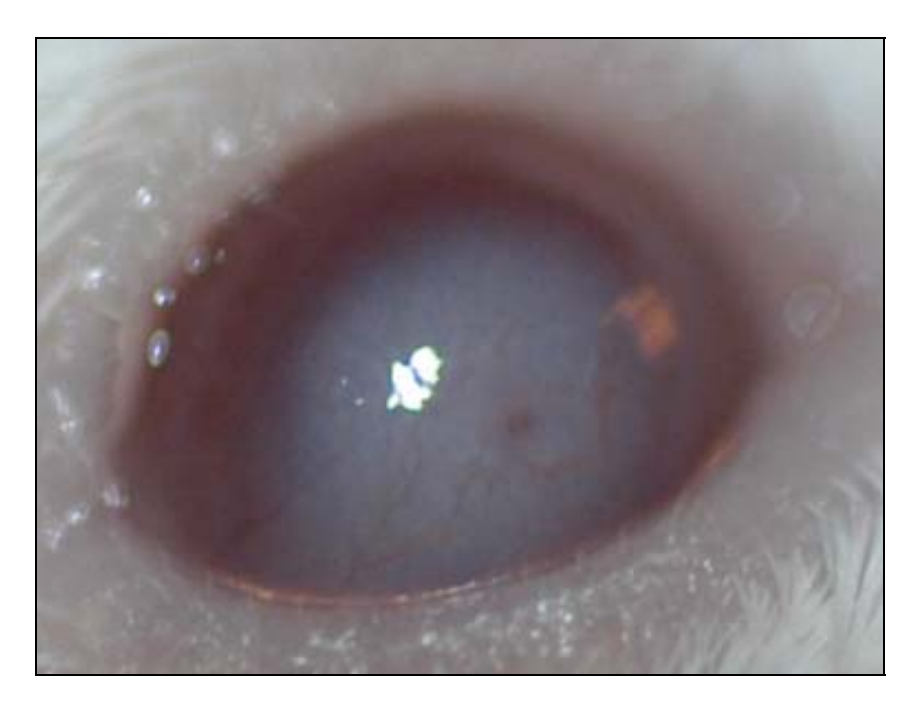
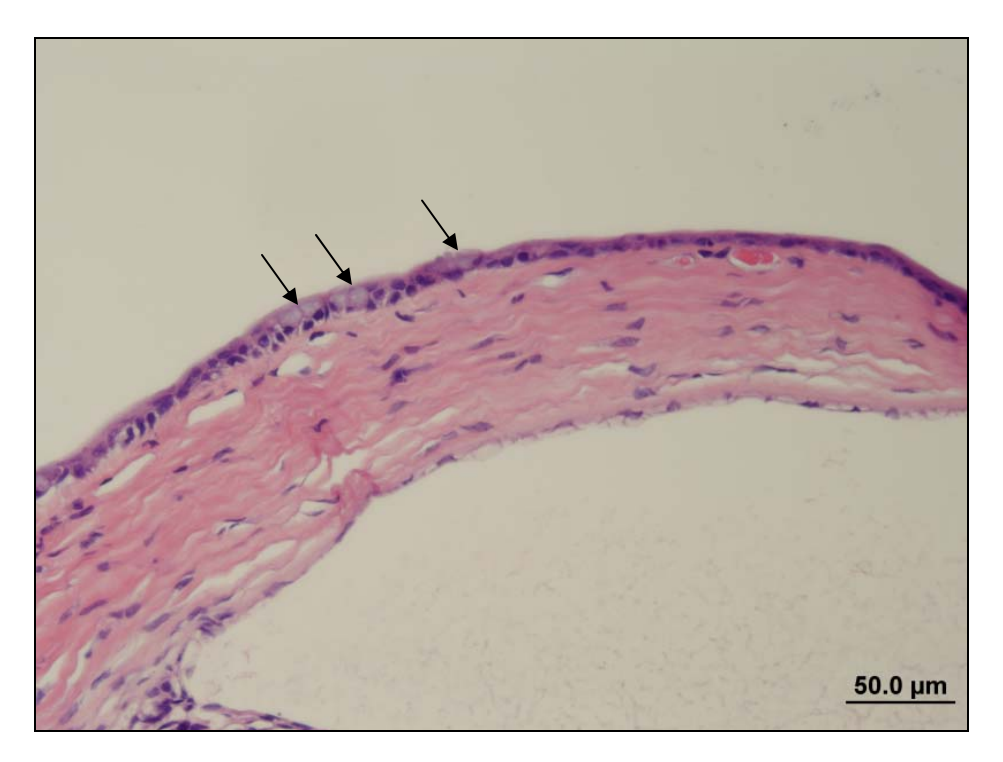




Figure 4: Representative clinical photograph (a) and corneal photomicrograph (b) of Sey mouse prior to wounding. In the clinical photograph, note the relative microophthalmia, corneal opacification and vascularization. Microscopically, the cornea was thicker than WT and was characterized by a thin (3-4 cell layers) squamous epithelium with a dense, disorganized, edematous, fibrovascular stroma.



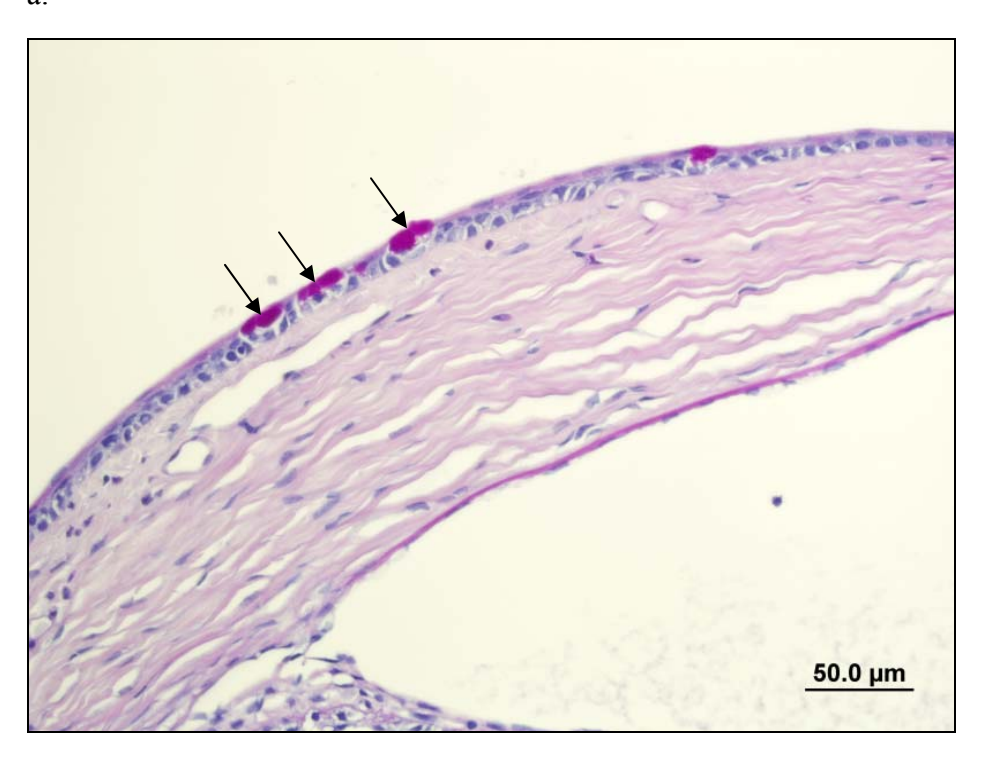
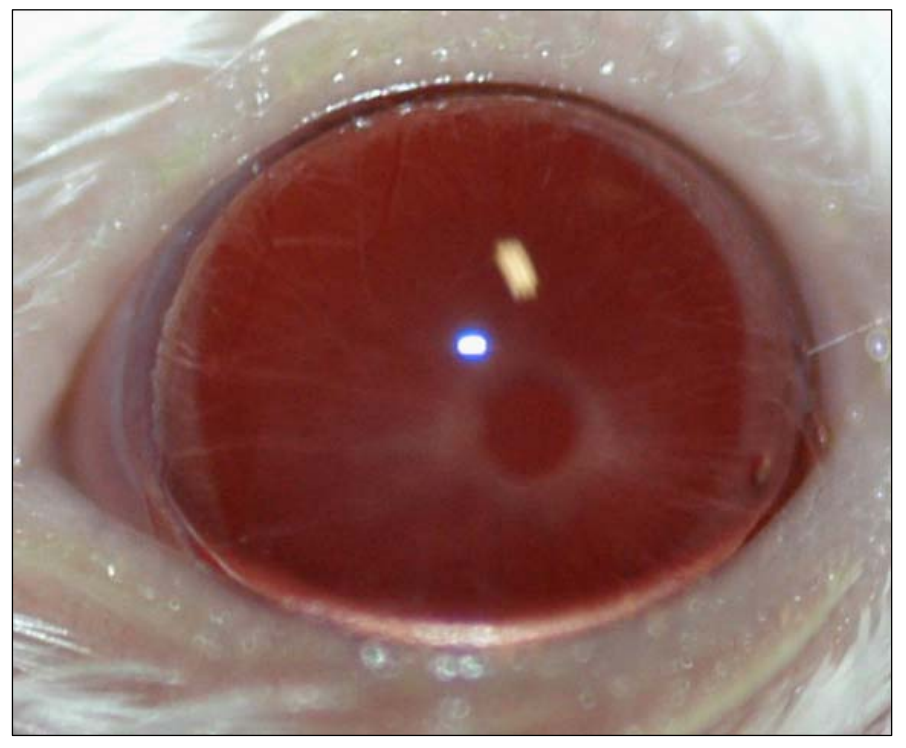


Figure 5: Photomicrograph of Sey cornea, showing a large, lightly basophilic cytoplasmic vacuole (arrows) within epithelial cells on staining with H&E (a) and same vacuole (arrows) staining positive with PAS (b).



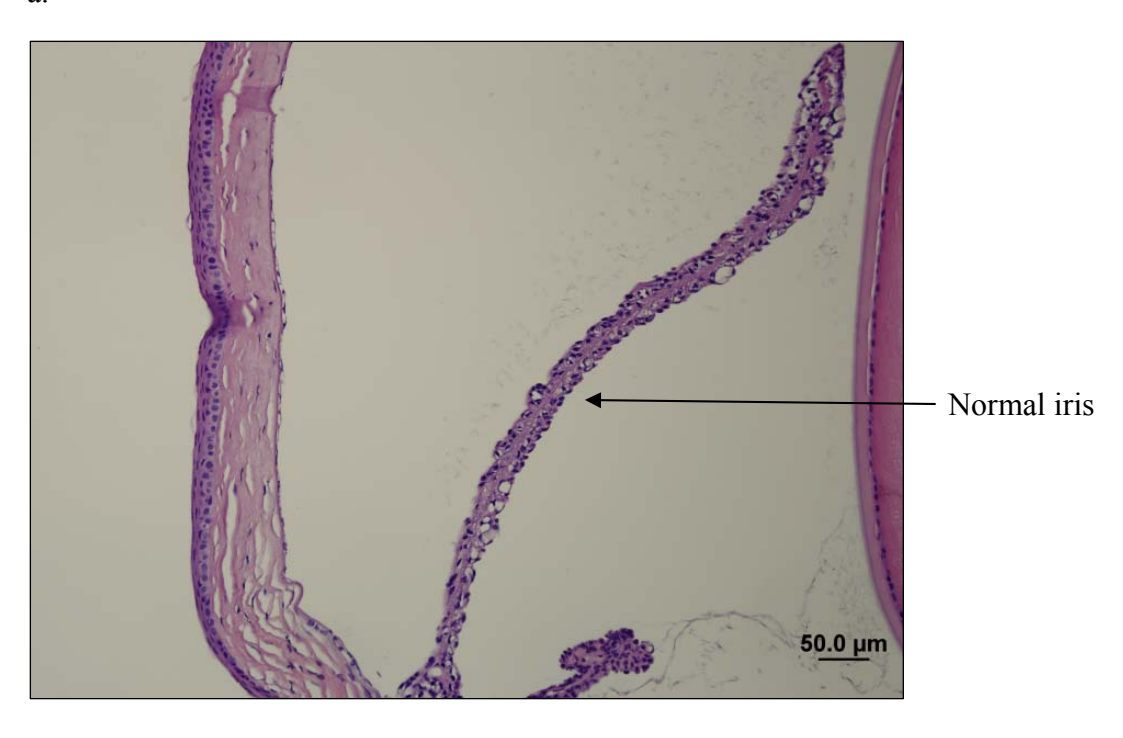
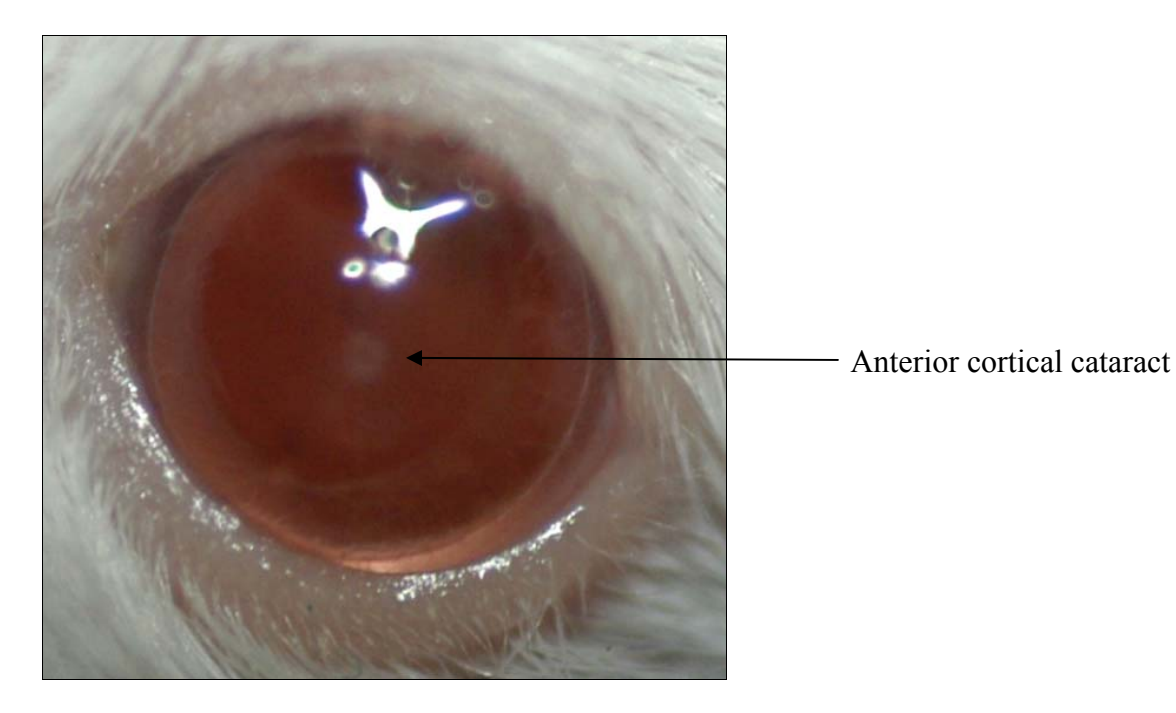


Figure 6: WT iris for subsequent Sey comparison. In the clinical photograph (a), note the normal appearing WT iris and circular, central pupil. In the photomicrograph (b), the WT iris is of normal size with an anterior and posterior epithelium, fibrovascular stroma, and smooth muscle.





Figure 7: Representative clinical photograph and photomicrograph of Sey anterior segment pathology. In the clinical photograph (a), note the iris hypoplasia with dyscoric pupil in this Sey mouse. In the photomicrograph (b), the Sey iris is hypoplastic with a lack of fibrovascular stroma and smooth muscle when compared to WT.



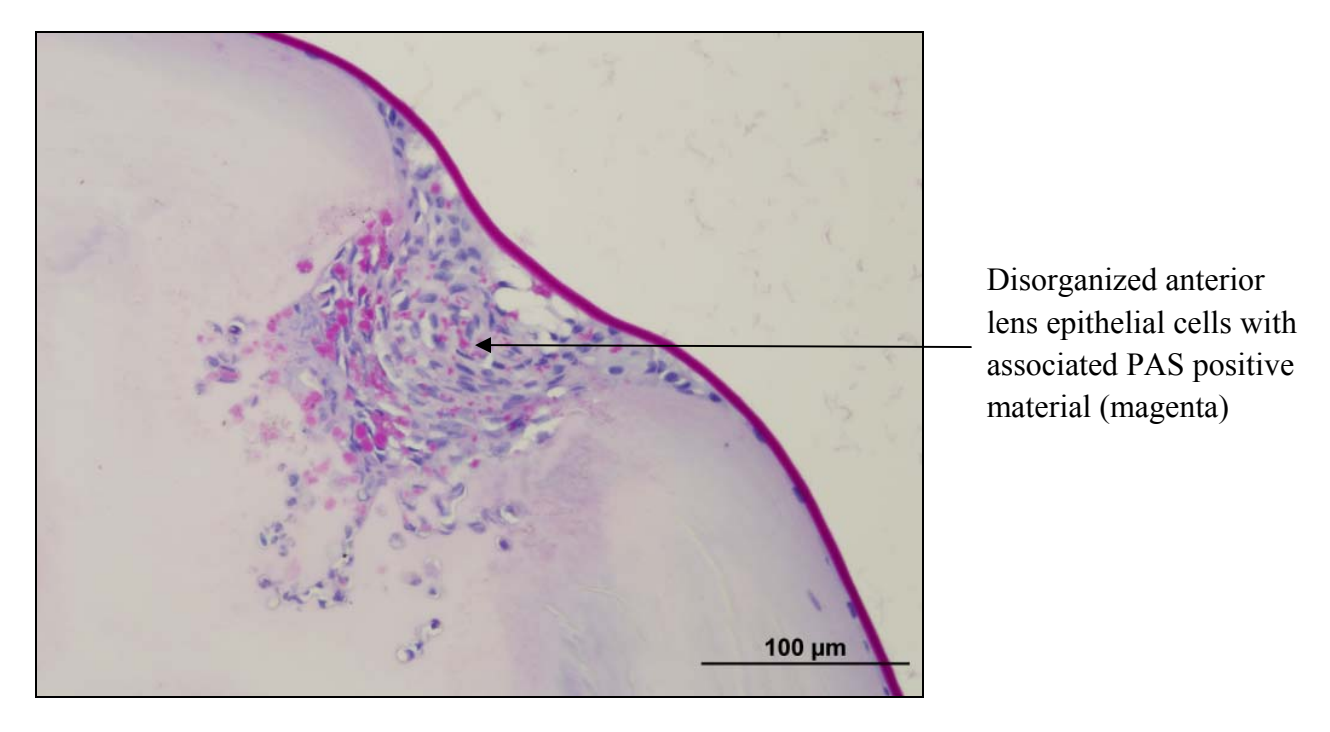


Figure 8: Representative clinical photograph and photomicrograph of Sey anterior segment pathology. In the clinical photograph (a), note the anterior cortical cataract. In the photomicrograph (b), the cataract is characterized by disorganized and proliferating anterior lens epithelial cells with associated PAS positive material. There is an intact overlying PAS positive lens capsule.



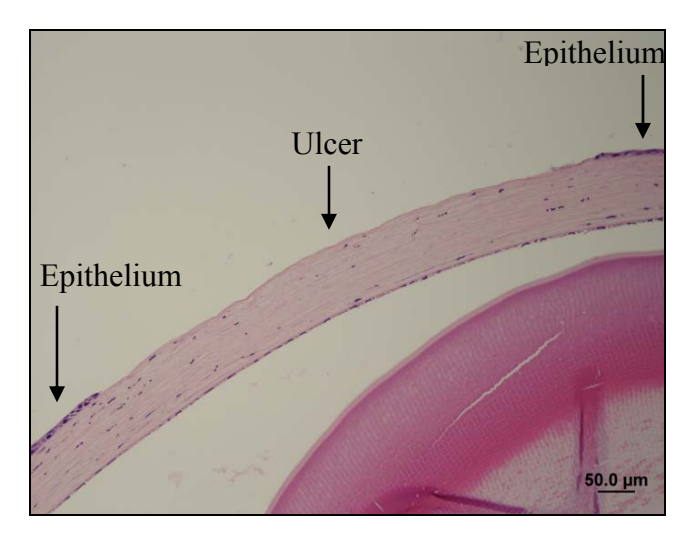


Figure 9: Clinical photograph and photomicrograph of Sey anterior segment pathology. In the clinical photograph (a), note the lens within the anterior chamber. In the photomicrograph (b), the anterior lens capsule is in contact with the posterior cornea. There is disorganization and proliferation of the anterior lens epithelial cells.





b.



c.

Figure 10: Representative wounding sequence showing application of n-heptanol saturated disk to central cornea (a), resultant fluorescein positive corneal ulcer (b), and corresponding histopathology (c).



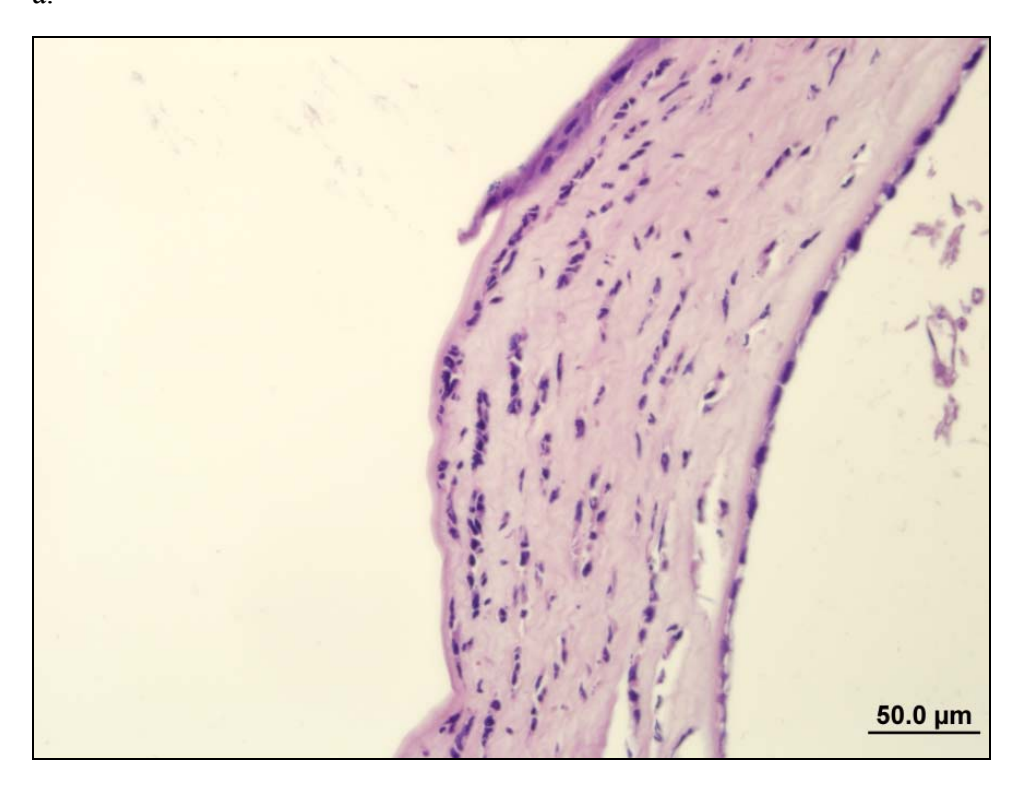


Figure 11: Photomicrograph of wounded WT (a) and Sey (b) cornea demonstrating a relative increase in stromal inflammatory cell infiltrate in the Sey group.

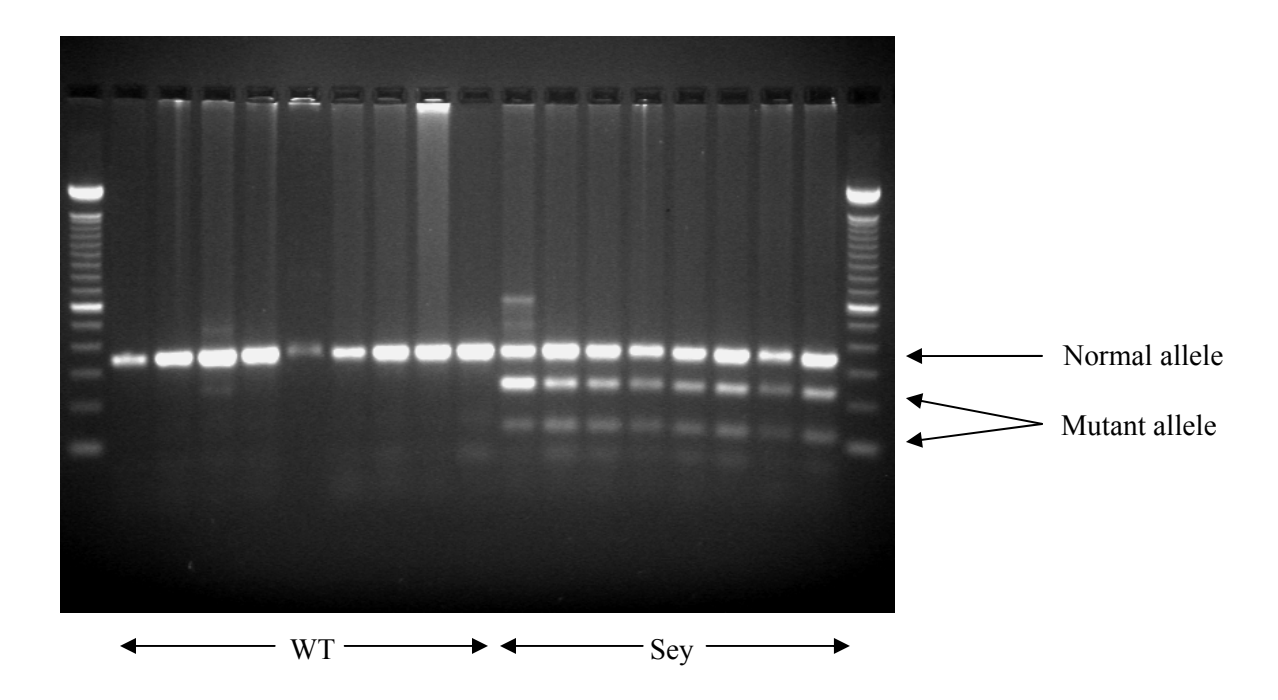
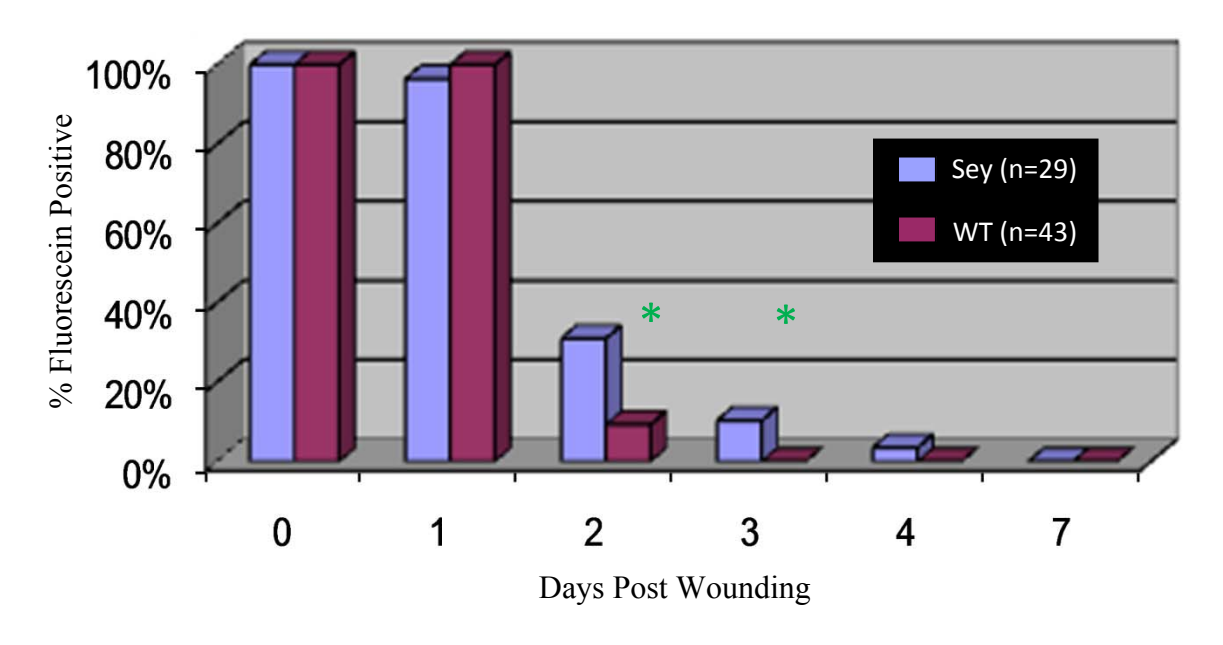


Figure 12: Murine genotype confirmation showing fractionated PCR products. Bands for WT show normal complement of Pax6, while bands for Sey demonstrate single normal Pax6 allele and characteristic two products of the HincII digestion (mutant allele).



\* Statistically significant difference (p<0.05)

Figure 13: Days to corneal healing after wounding with n-heptanol. All mice were fluorescein positive on day 0. There was a statistically significant delay in wound healing between groups on days 2 and 3. All mice were healed by day 7.

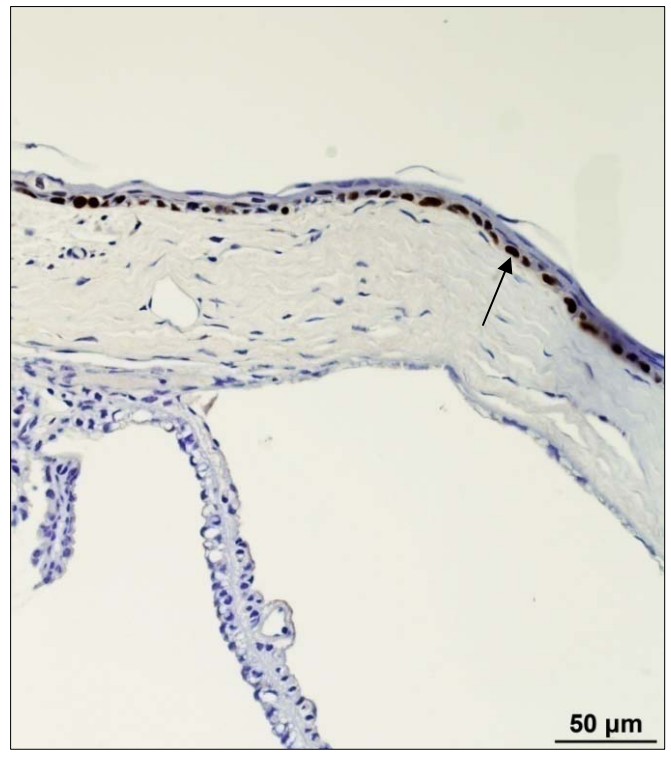
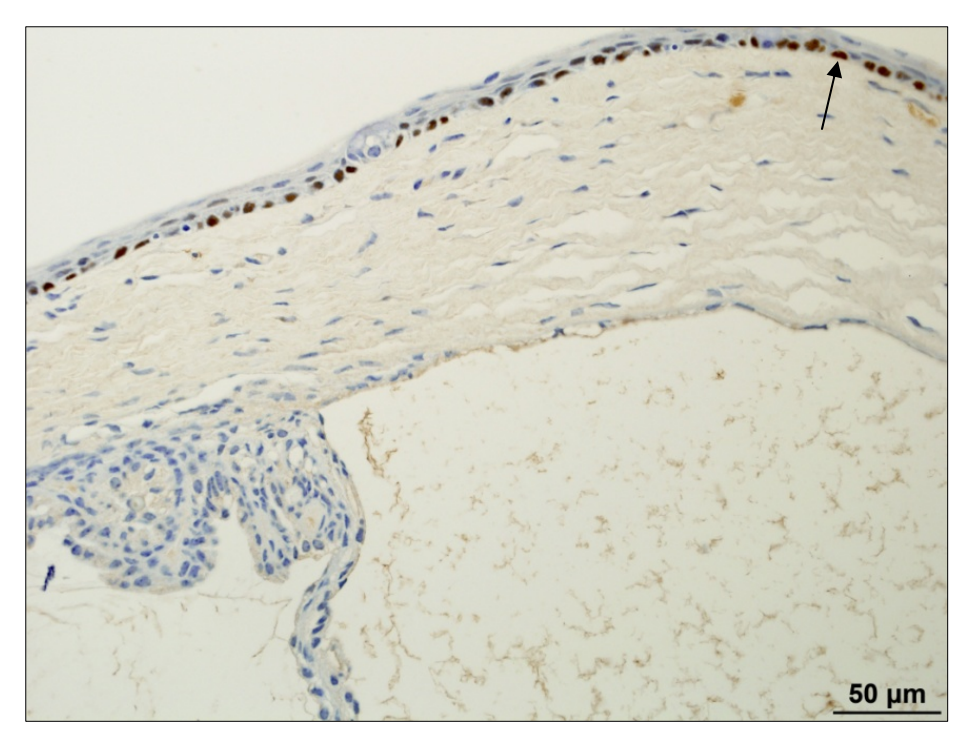




Figure 14: Expression of p63 in the epithelium of WT mice. Positive staining (brown) in each slide is nuclei of basal epithelial cells (arrow). Representative image (a,b) with different magnification show staining in non-wounded WT mice on day 1.



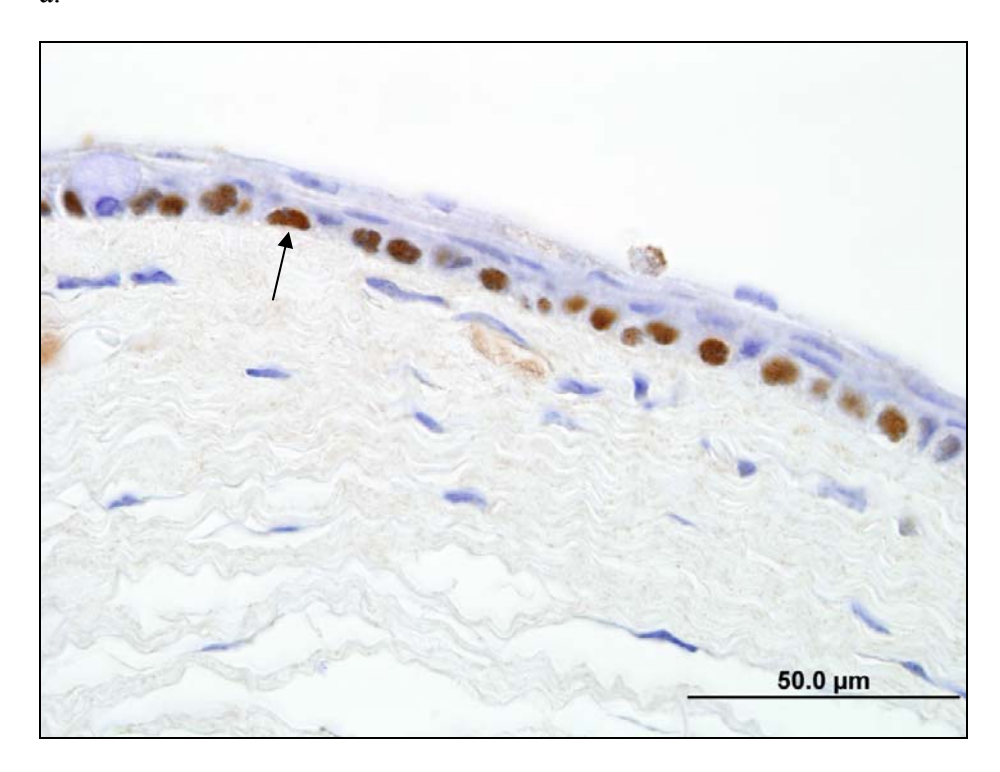
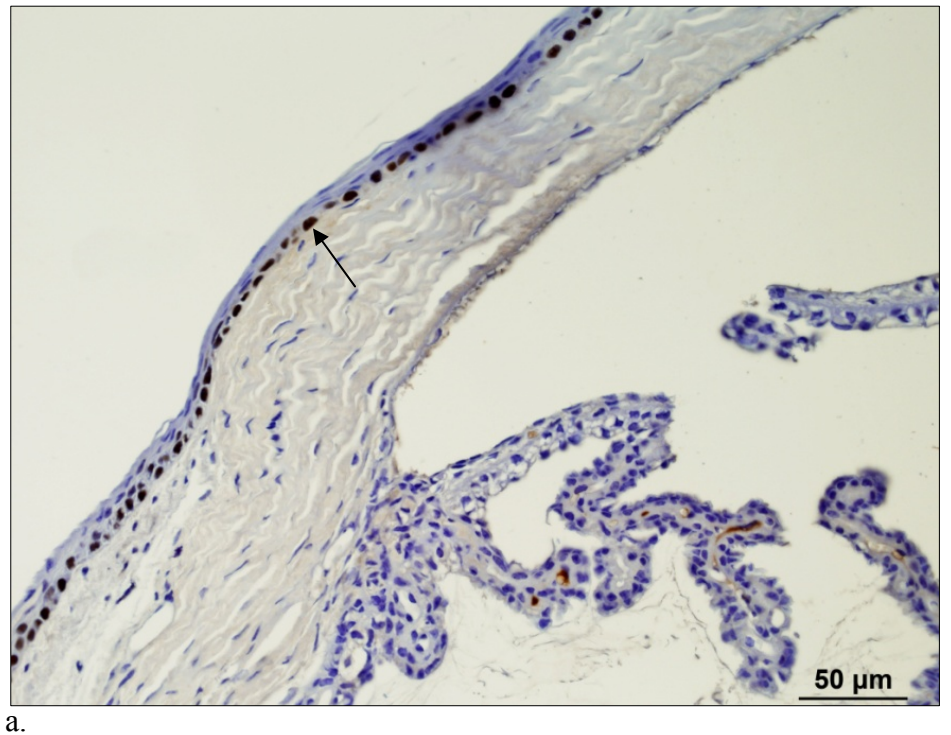


Figure 15: Expression of p63 in the epithelium of Sey mice. Positive staining (brown) in each slide is nuclei of basal epithelial cells (arrow). Representative image (a,b) with different magnification show staining in non-wounded Sey mice on day 1.



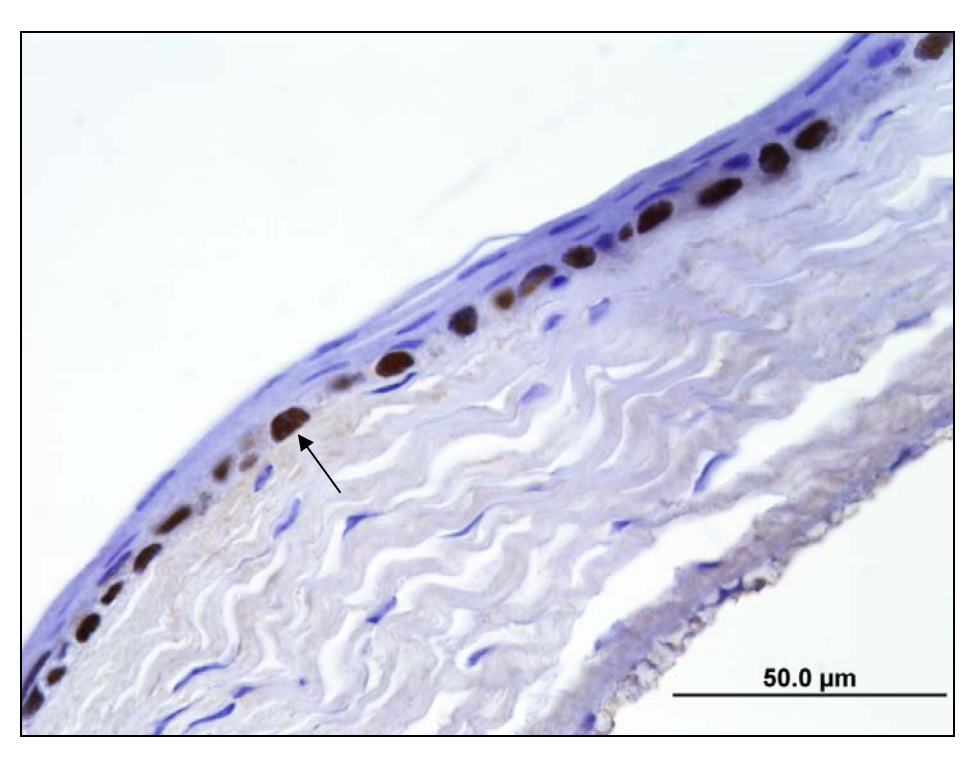
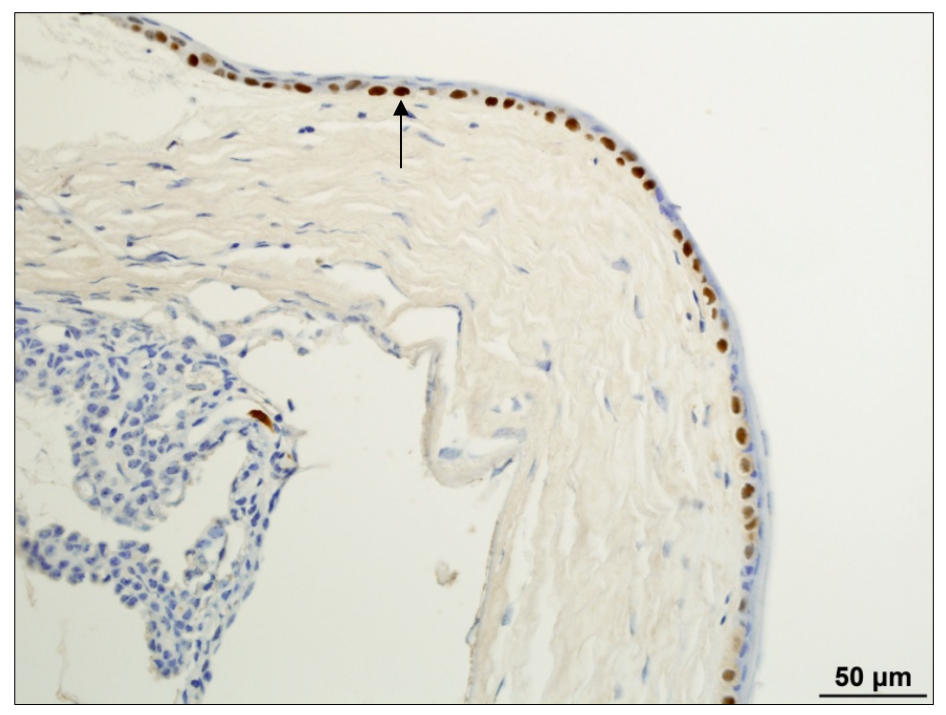


Figure 16: Expression of p63 in the epithelium of WT mice. Positive staining (brown) in each slide is nuclei of basal epithelial cells (arrow). Representative image (a,b) with different magnification show staining in WT mice on post wounding day 28.



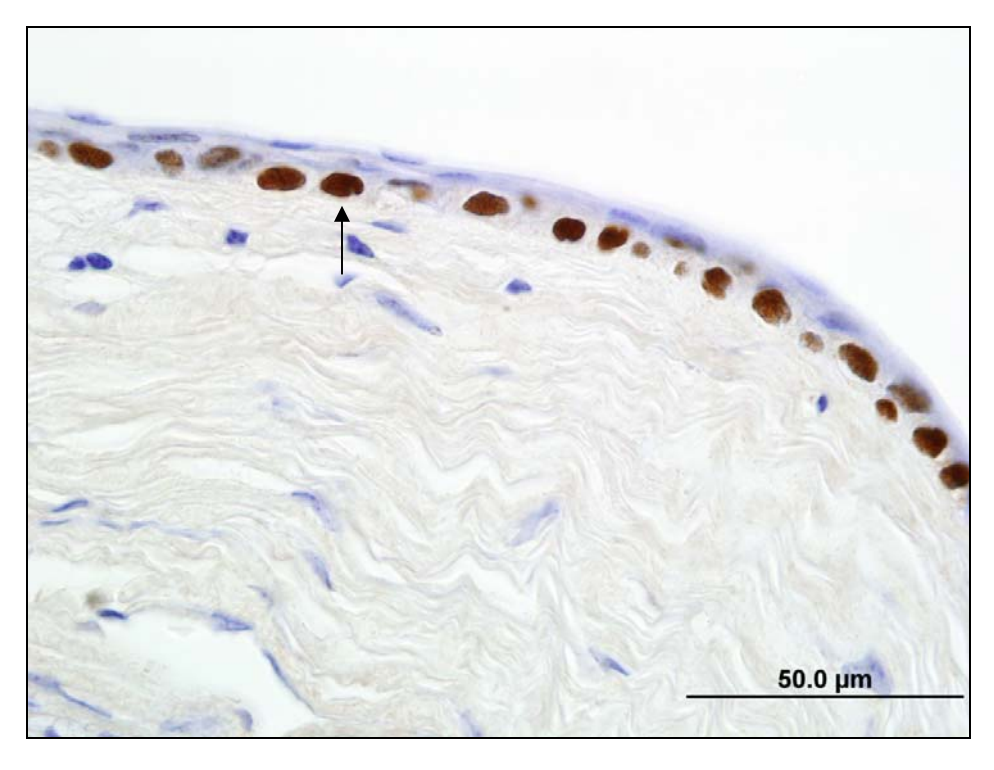


Figure 17: Expression of p63 in the epithelium of Sey mice. Positive staining (brown) in each slide is nuclei of basal epithelial cells (arrow). Representative image (a,b) with different magnification show staining in Sey mice on post wounding day 28.

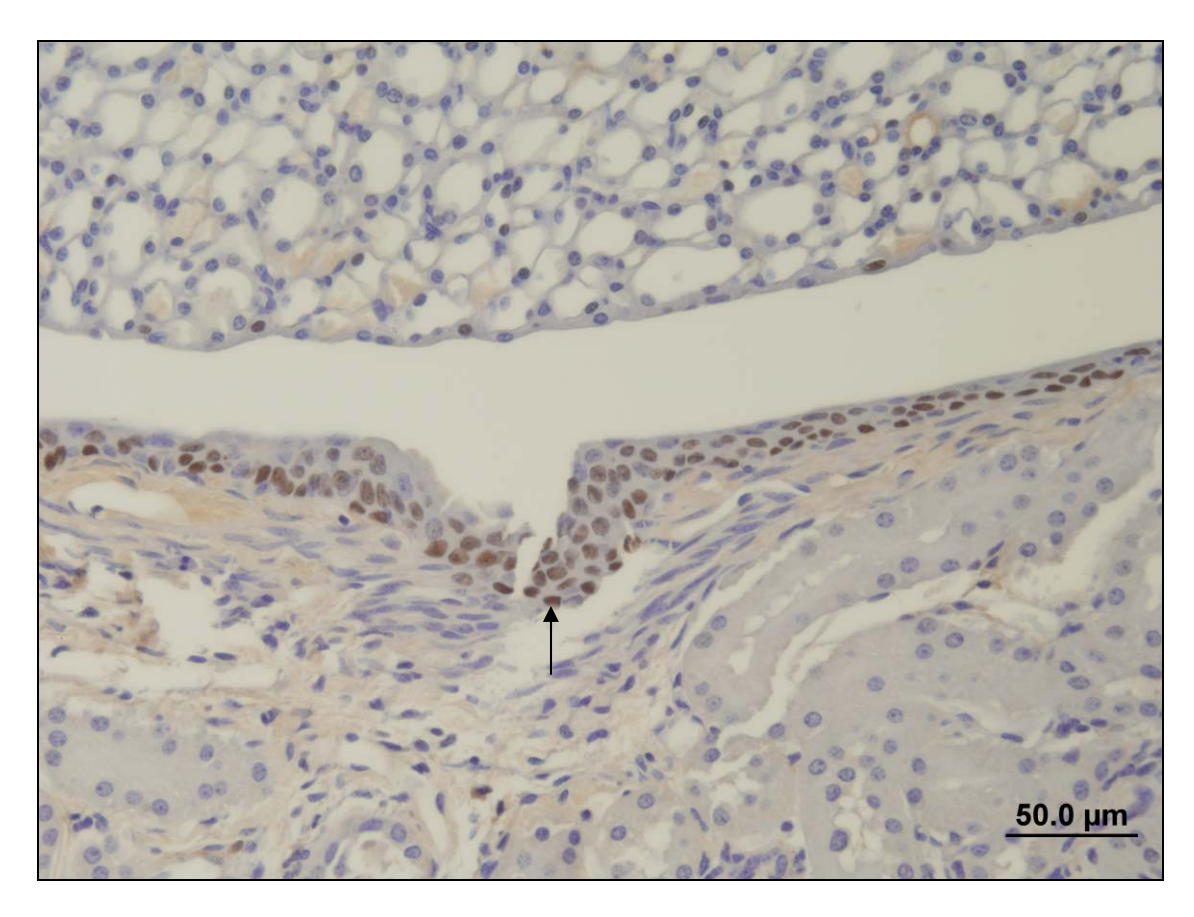


Figure 18: Photomicrograph of mouse renal pelvis showing p63 positive control. As expected, the transitional epithelium is positive for p63 (brown nuclear staining; arrow).

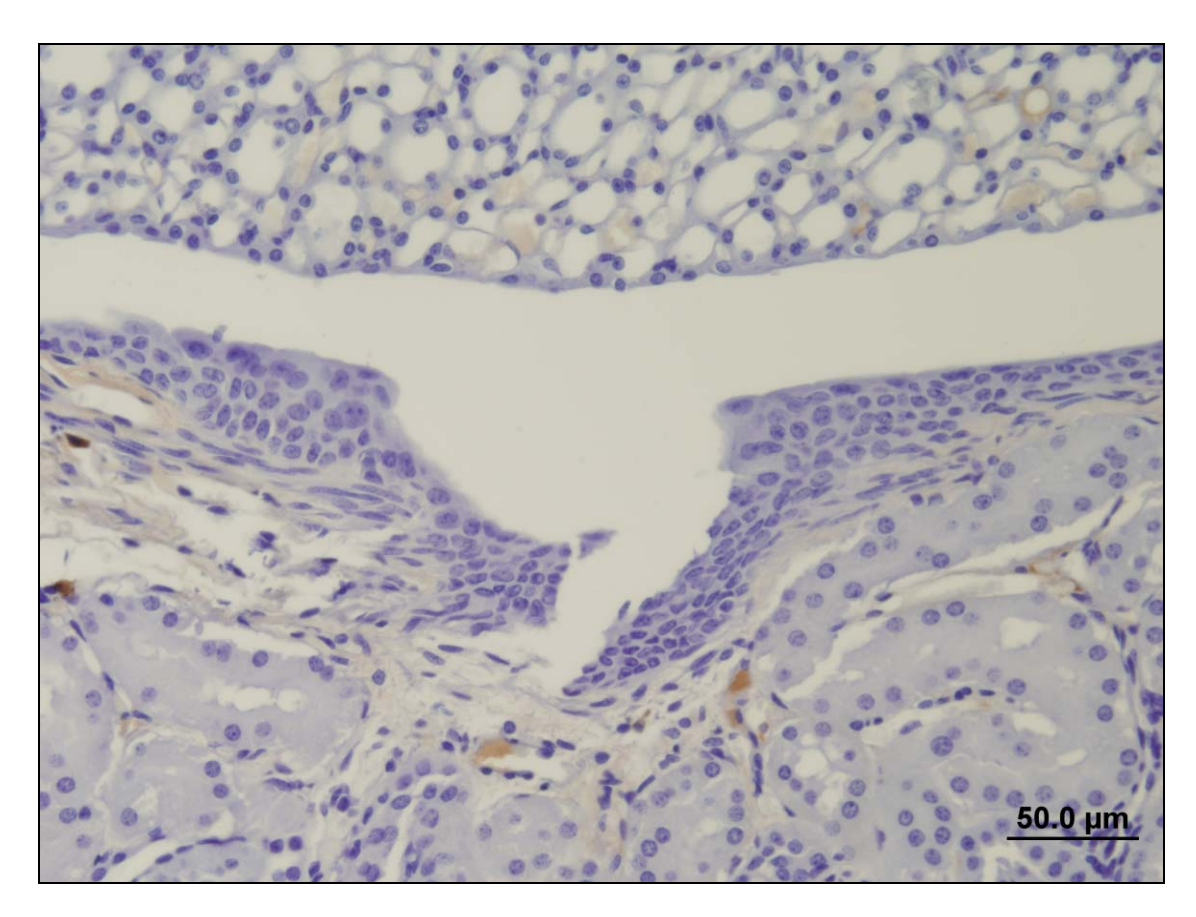


Figure 19: Photomicrograph of mouse renal pelvis showing p63 negative control (normal horse serum). As expected, the transitional epithelium is devoid of staining.

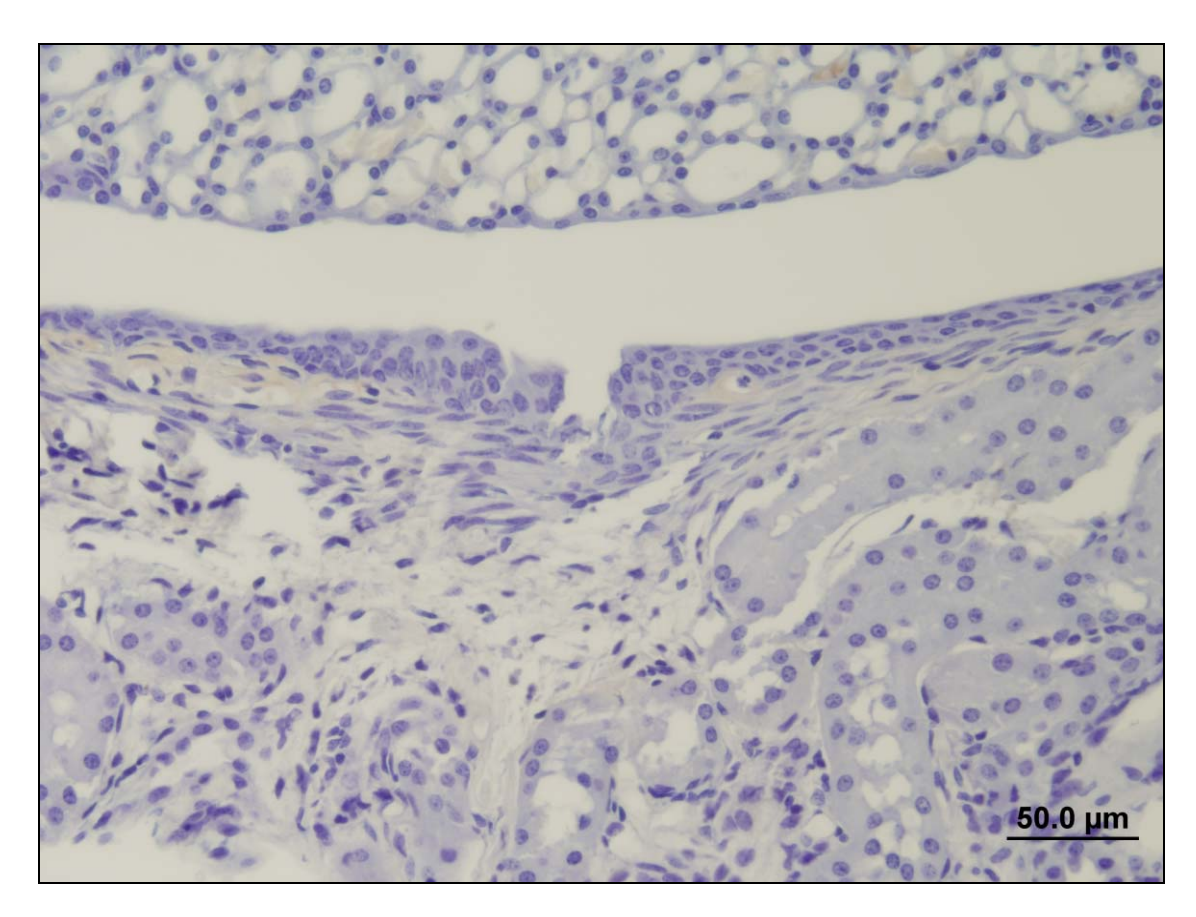
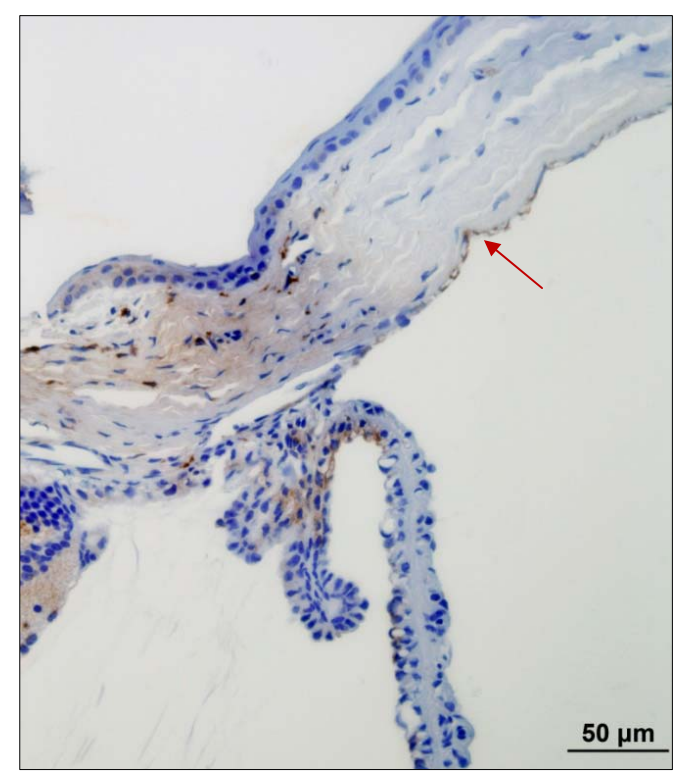


Figure 20: Photomicrograph of mouse renal pelvis showing p63 negative control (PBS). As expected, the transitional epithelium is devoid of staining.



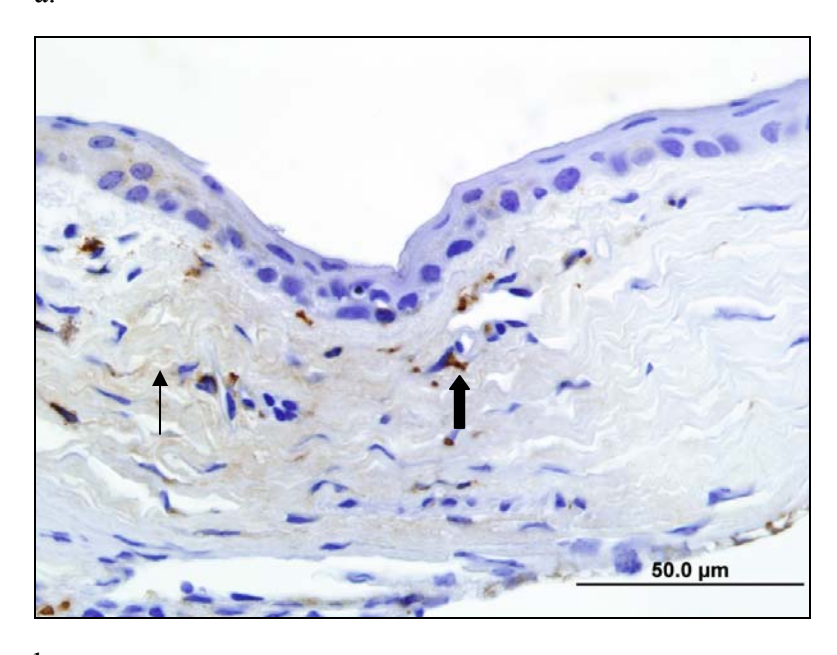
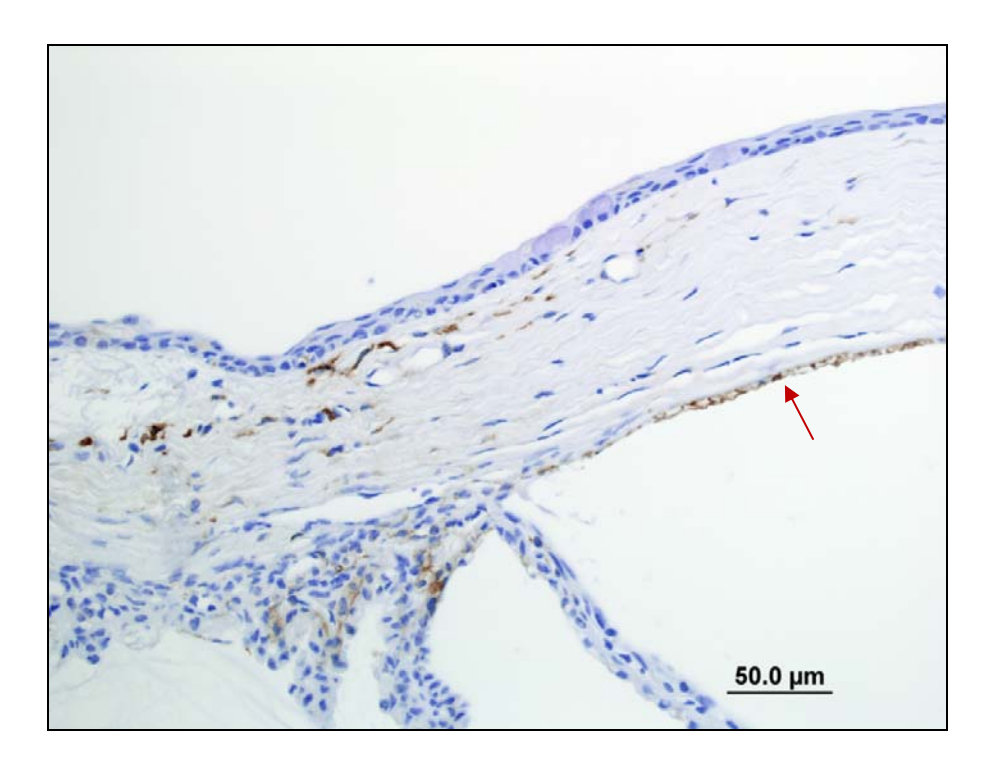


Figure 21: Expression of sVEGFR-1 in non-wounded WT mice. Positive staining in each slide is brown. Representative image (a,b) with different magnification show staining in non-wounded WT mice on day 1 (red arrow = endothelial staining; block arrow = keratocyte staining; thin arrow = stromal staining).



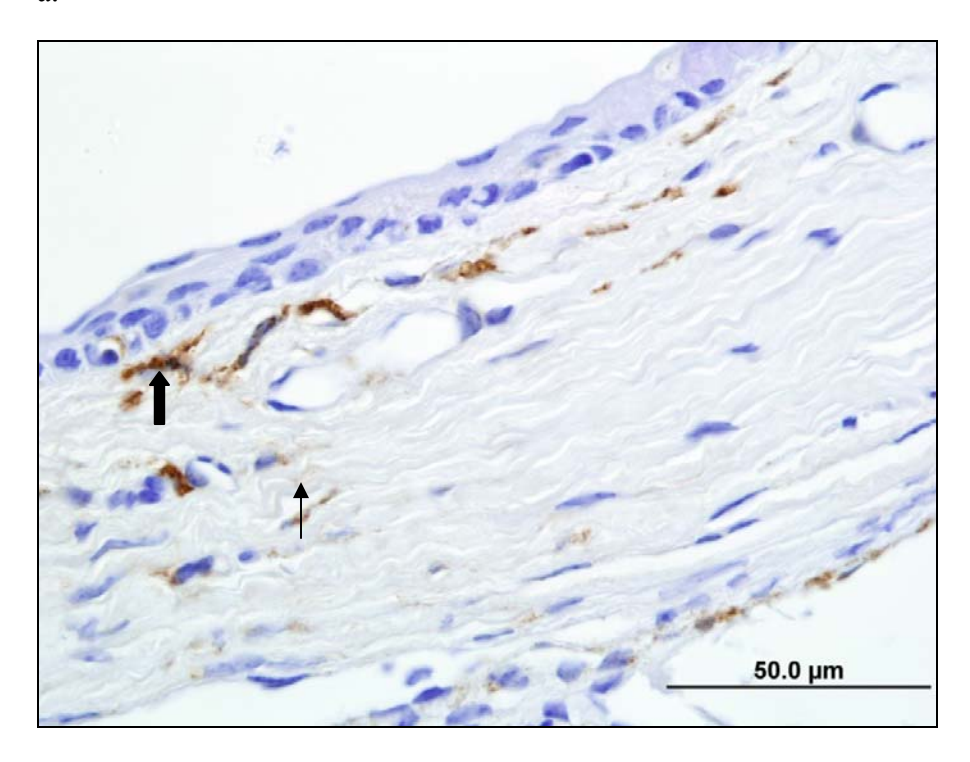


Figure 22: Expression of sVEGFR-1 in non-wounded Sey mice. Positive staining in each slide is brown. Representative image (a,b) with different magnification show staining in non-wounded Sey mice on day 1 (red arrow = endothelial staining; block arrow = keratocyte staining; thin arrow = stromal staining).

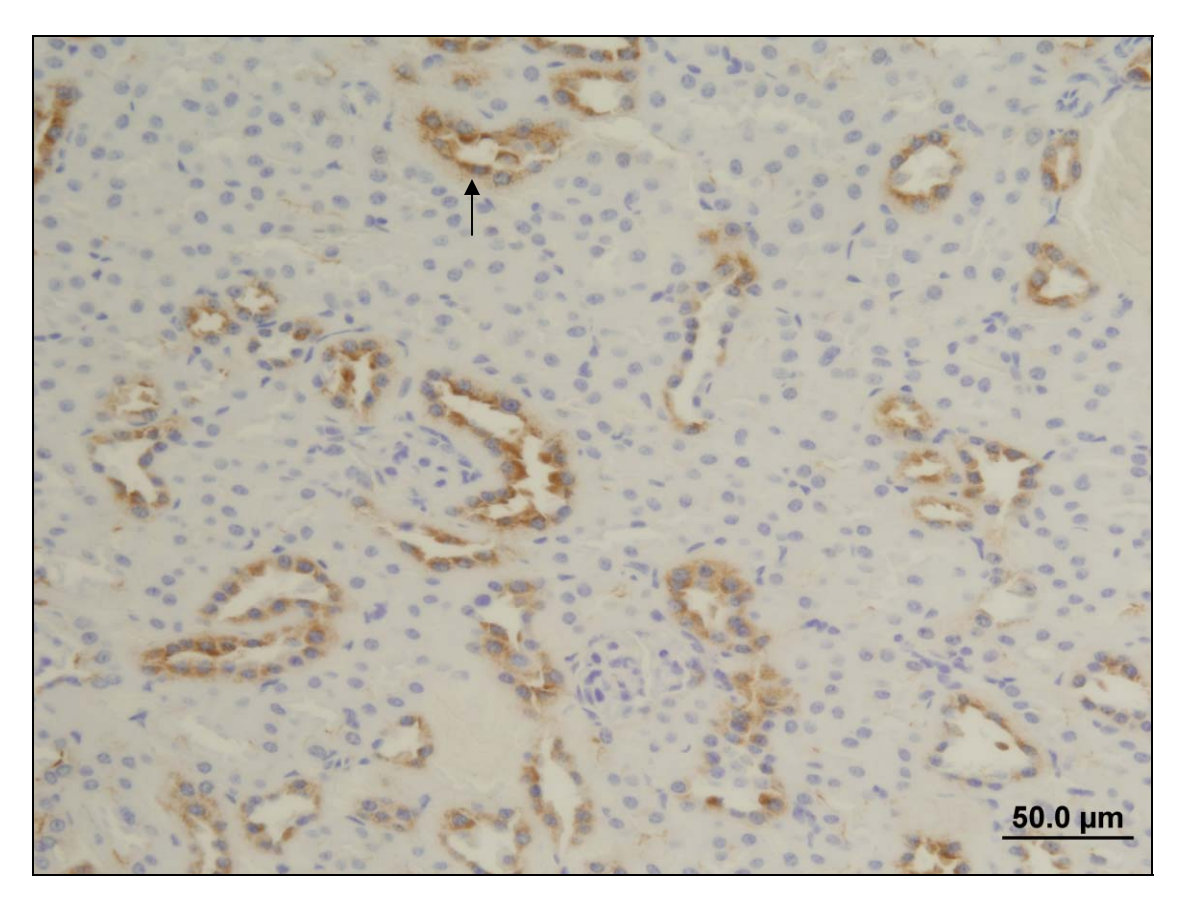


Figure 23: Photomicrograph of mouse kidney showing sVEGFR-1 positive control. As expected, the proximal tubular cells are positive for sVEGFR-1 (brown staining; arrow).

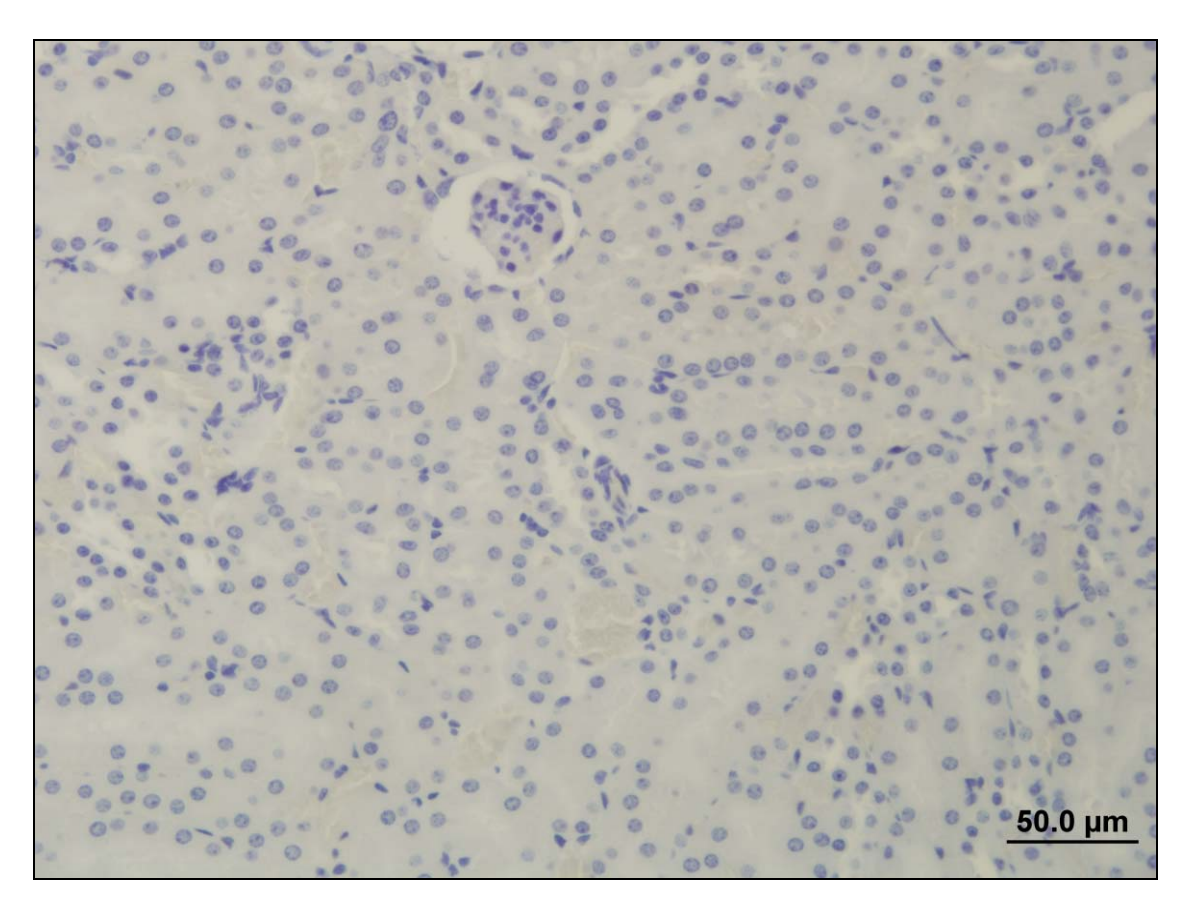


Figure 24: Photomicrograph of mouse kidney showing sVEGFR-1 negative control (normal rat serum). As expected, the proximal tubular cells are devoid of staining.

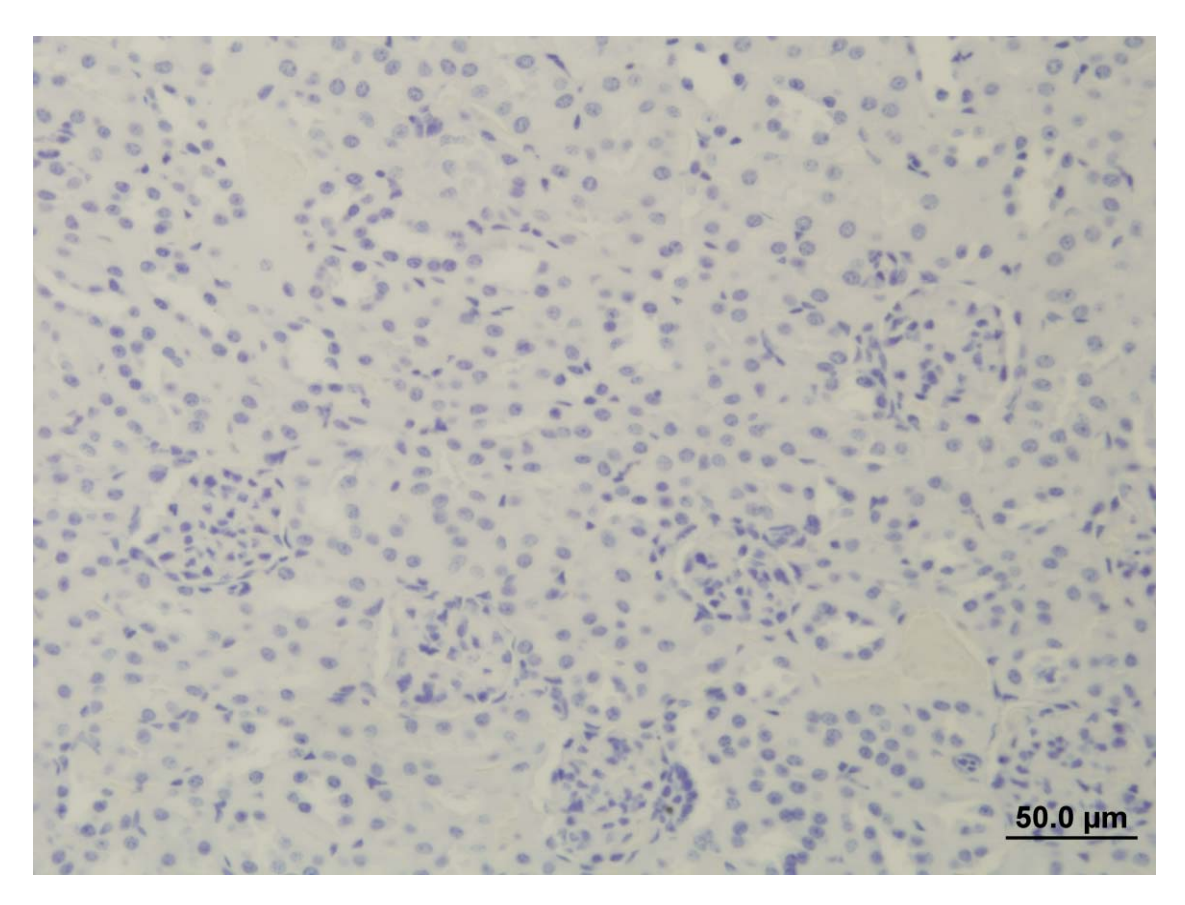
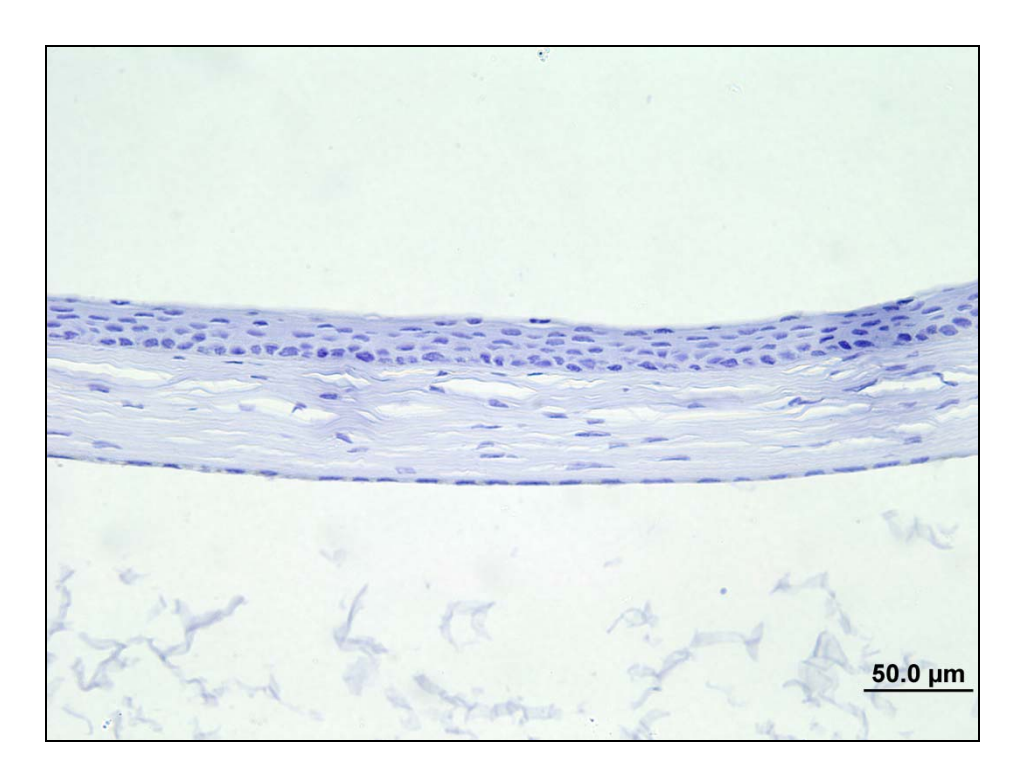


Figure 25: Photomicrograph of mouse kidney showing sVEGFR-1 negative control (PBS). As expected, the proximal tubular cells are devoid of staining.



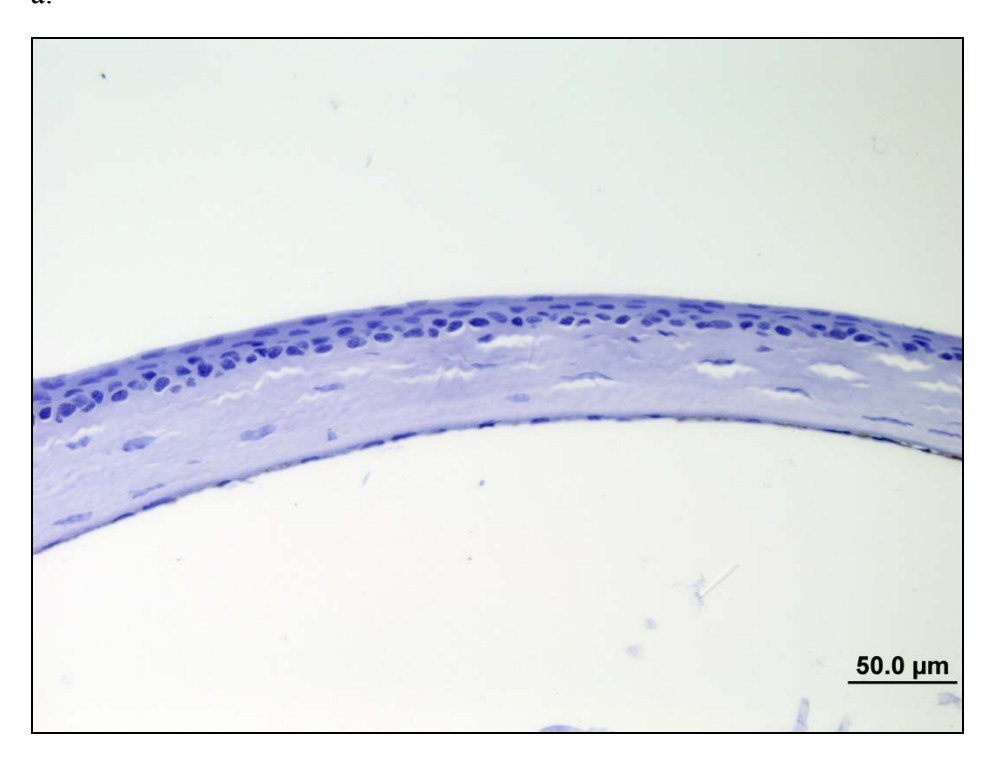
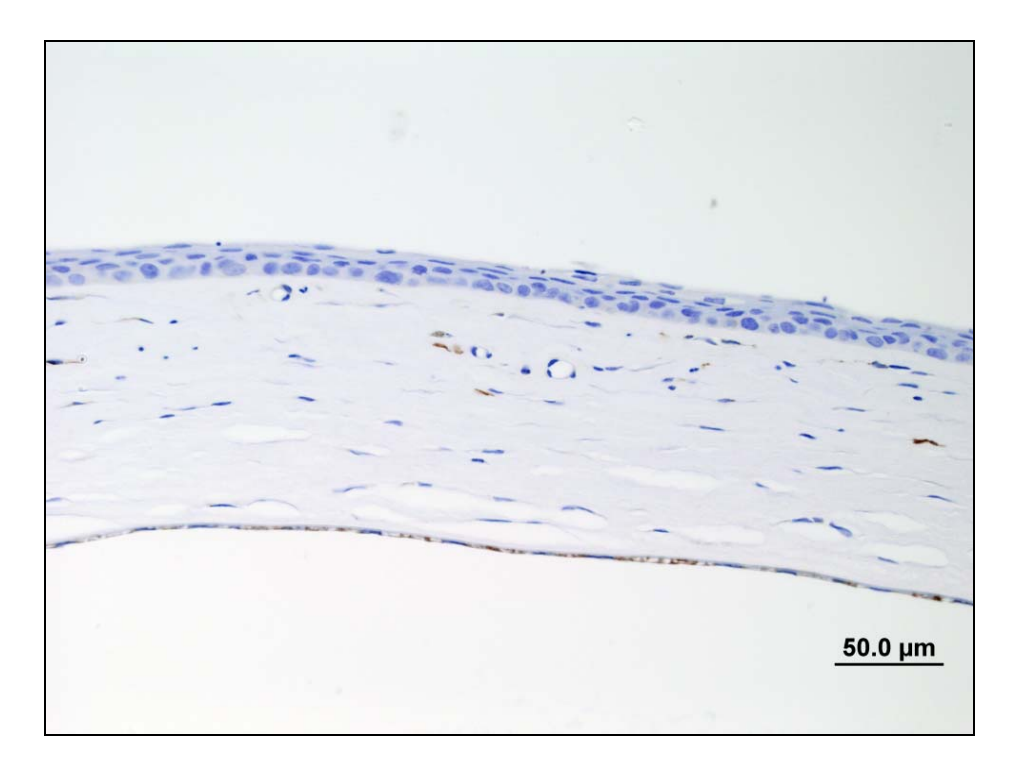


Figure 26: Immunohistochemistry for sVEGFR-1 in central cornea. There was no sVEGFR-1 staining within the central corneal epithelium or stroma in non-wounded WT eyes (a) and the majority of Sey eyes (b).



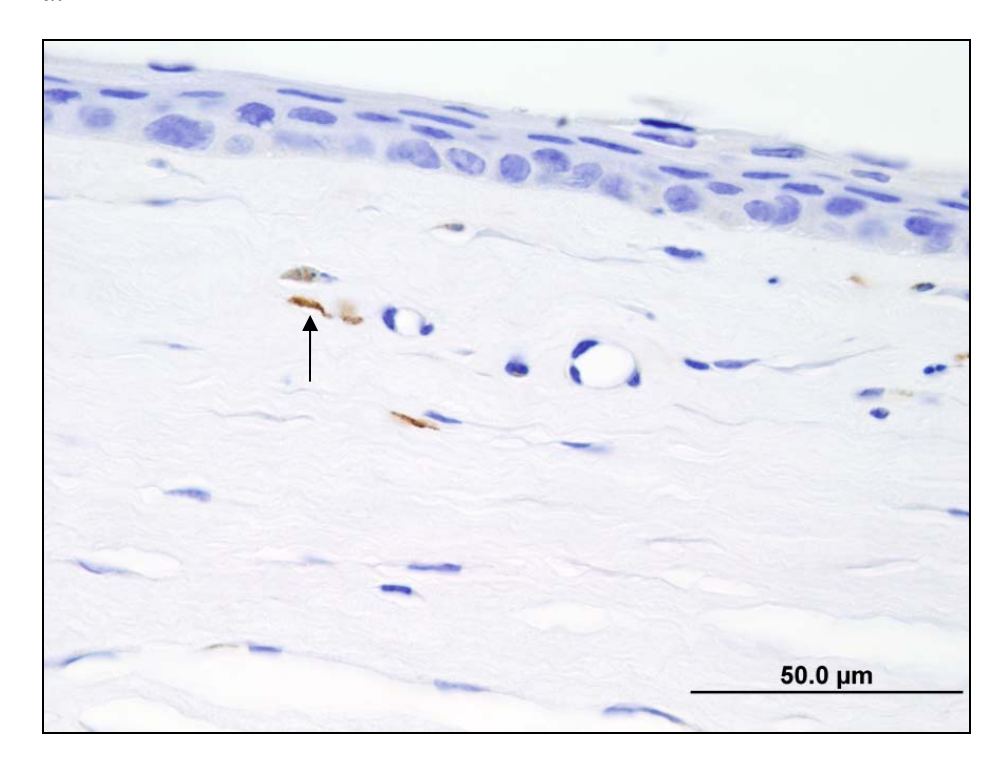


Figure 27: Immunohistochemistry for sVEGFR-1 in central cornea. In the Sey group, a total of 8 mice (33%) had staining within the central corneal stroma (a,b). Keratocyte staining is indicated (arrow).

## CHAPTER 3

## **CONCLUSION**

The results of this study have shown precise and accurate corneal epithelial removal with n-heptanol in an *in vivo* model using WT and Sey mice. This model has confirmed an inherent deficiency in corneal wound healing in the Sey mouse that is likely partly responsible for the ARK phenotype. While additional study is needed, the wound healing deficiency observed in Sey mice did not appear to be caused by depletion in the limbal progenitor cell population (p63 expressing cells). Localization of p63 within the wing cells and superficial cells of the cornea suggests an impairment of epithelial cell differentiation and further study is needed to evaluate the significance of this finding. Comparable anatomic localization of sVEGFR-1 suggests a role for this factor in the maintenance of corneal avascularity. However, given the results reported here, it is unlikely that this factor alone is responsible for the prominent corneal vascularization in Sey mice. This wounding paradigm provides an option for future in vivo evaluation of corneal pathophysiology in Pax6 deficiency and a model for testing and comparing potential therapeutic intervention. Further characterization of the epithelial and stromal pathology, including limbal stem cell function, in Sey mice may lead to therapeutic strategies (corrective gene therapy) in the future.